# Machine Learning Techniques for Gesture Recognition

Carlos Antonio Caceres

Thesis submitted to the faculty of the Virginia Polytechnic Institute and State University
in partial fulfillment of the requirements for the degree of

Master of Science
In
Mechanical Engineering

Alfred L. Wicks, Chair
John P. Bird
Craig A. Woolsey

September 9th, 2014
Blacksburg, VA

Keywords: Gesture Recognition, Smart Prosthetic, Hidden Markov Model, Support Vector Machines, Dynamic Time Warping

# Machine Learning Techniques for Gesture Recognition

Carlos Antonio Caceres

## ABSTRACT

Classification of human movement is a large field of interest to Human-Machine Interface researchers. The reason for this lies in the large emphasis humans place on gestures while communicating with each other and while interacting with machines. Such gestures can be digitized in a number of ways, including both passive methods, such as cameras, and active methods, such as wearable sensors. While passive methods might be the ideal, they are not always feasible, especially when dealing in unstructured environments. Instead, wearable sensors have gained interest as a method of gesture classification, especially in the upper limbs. Lower arm movements are made up of a combination of multiple electrical signals known as Motor Unit Action Potentials (MUAPs). These signals can be recorded from surface electrodes placed on the surface of the skin, and used for prosthetic control, sign language recognition, human machine interface, and a myriad of other applications.

In order to move a step closer to these goal applications, this thesis compares three different machine learning tools, which include Hidden Markov Models (HMMs), Support Vector Machines (SVMs), and Dynamic Time Warping (DTW), to recognize a number of different gestures classes. It further contrasts the applicability of these tools to noisy data in the form of the Ninapro dataset, a benchmarking tool put forth by a conglomerate of universities. Using this dataset as a basis, this work paves a path for the analysis required to optimize each of the three classifiers. Ultimately, care is taken to compare the three classifiers for their utility against noisy data, and a comparison is made against classification results put forth by other researchers in the field.

The outcome of this work is 90+ % recognition of individual gestures from the Ninapro dataset whilst using two of the three distinct classifiers. Comparison against previous works by other researchers shows these results to outperform all other thus far. Through further work with these tools, an end user might control a robotic or prosthetic arm, or translate sign language, or perhaps simply interact with a computer.

# Dedication

For my family.

# Acknowledgements

I'd like to use these lines to thank all those people who helped get me to this point. Graduate school has been an amazing journey, where I have learned more than I could've hoped for, met some of the brightest and best people I know, and ultimately grown as a person and an engineer.

Particular thanks go to my committee members, without whom the last two years would have been a much more difficult path. First, Dr. Craig Woolsey, whose help and kindness in my early days at Virginia Tech helped guide me towards the kind of research I wanted to follow. Second, Dr. John Bird who has been a constant source of wisdom and guidance during my time as a graduate student. And finally, my sincerest appreciation and respect to Dr. Al Wicks. Without the opportunities and support of Dr. Wicks, graduate school would have been a constant struggle. For these reasons and many more, these three men have earned my lifelong respect and appreciation.

Finally, I must thank my parents, who have worked extremely hard since arriving in this country, all for the benefit of their children.

# Table of Contents

Dedication ..... iii
Acknowledgements ..... iv
Table of Contents ..... v
List of Figures ..... viii
List of Tables ..... x
Acronyms ..... x
1 Introduction ..... 1
1.1 Background Problem ..... 1
1.2 Proposed Solution ..... 4
1.3 Thesis Structure ..... 4
1.4 Summary ..... 5
2 Literature Review ..... 7
2.1 Chapter Summary ..... 7
2.2 Previous Research ..... 7
2.3 Summary ..... 11
3 Background Theory ..... 12
3.1 Chapter Summary ..... 12
3.2 Electromyography ..... 12
3.3 Physiology ..... 14
3.4 Machine Learning ..... 15
3.4.1 Hidden Markov Models ..... 16
3.4.2 Dynamic Time Warping ..... 19
3.4.3 Support Vector Machine ..... 23
3.5 Summary ..... 24
4 Methods ..... 26
4.1 Chapter Summary ..... 26
4.2 Dataset ..... 26
4.3 Active Segments ..... 29

4.4 Feature Extraction ..... 30
4.5 Feature Selection ..... 33
4.6 Hidden Markov Models ..... 36
4.6.1 Vector Discretization ..... 37
4.6.2 Model Setup ..... 38
4.6.3 Left to Right vs. Ergodic Models ..... 39
4.6.4 Effect of Increasing Vocabulary ..... 39
4.6.5 Minimum Required Training Data ..... 40
4.6.6 Optimized Model ..... 40
4.7 Support Vector Machines ..... 42
4.7.1 Data Scaling ..... 43
4.7.2 Kernel Test ..... 44
4.7.3 Effect of Increasing Vocabulary ..... 44
4.7.4 Minimum Required Training Data ..... 44
4.7.5 Optimized Model ..... 45
4.8 Dynamic Time Warping ..... 45
4.8.1 Data Preparation ..... 46
4.8.2 Threshold calculation ..... 46
4.8.3 Optimized Model ..... 47
4.9 Summary ..... 47
5 Results ..... 49
5.1 Chapter Summary ..... 49
5.2 Optimal Data and Feature Representation ..... 50
5.2.1 Feature Threshold ..... 50
5.2.2 Number of frames ..... 52
5.2.3 Filter method feature selection ..... 53
5.2.4 Hidden Markov Model Wrapper ..... 54
5.2.5 Support Vector Machine Wrapper ..... 55
5.3 Dynamic Time Warping Results ..... 56
5.3.1 Number of Examples and Data Preparation Test ..... 56
5.3.2 Final Model ..... 58

5.3.3 Issues with Dynamic Time Warping Method ..... 60
5.4 Hidden Markov Model Results ..... 62
5.4.1 Model Setup ..... 62
5.4.2 Left to Right vs. Ergodic Models ..... 63
5.4.3 Effect of Increasing Vocabulary ..... 64
5.4.4 Minimum Required Training Data ..... 65
5.4.5 Final Feature Model ..... 66
5.4.6 Final SAX Model ..... 69
5.5 SVM Results ..... 72
5.5.1 Kernel Test ..... 73
5.5.2 Effect of Increasing Vocabulary ..... 74
5.5.3 Minimum Required Training Data ..... 75
5.5.4 Final SVM Model ..... 75
5.6 Summary ..... 77
6 Conclusions ..... 78
6.1 Chapter Summary ..... 78
6.2 Previous Ninapro Results ..... 78
6.3 Thesis Results ..... 79
6.4 Achievement ..... 81
6.5 Future work ..... 82
6.6 Summary ..... 83
References ..... 84
Appendix A: Gesture Dictionary ..... 89
Appendix B: EMG Features ..... 91

# List of Figures

Figure 1: ASL Hand Signs [1] ..... 2
Figure 2: SWAT Team Hand Signs [2] ..... 2
Figure 3: Control Strategy for Smart Prosthetics [8] ..... 3
Figure 4: The Motor Unit [26] ..... 12
Figure 5: Motorneuron's EMG Signal Generation [25] ..... 13
Figure 6: Forearm Muscle Groups [27] ..... 15
Figure 7: HMM Topologies, left to right (top) and ergodic (bottom) [17] ..... 17
Figure 8: DTW Method [31] ..... 20
Figure 9: DTW Optimal Warping Path [31] ..... 21
Figure 10: DTW Classification Process [17] ..... 22
Figure 11: SVM Margin [17] ..... 23
Figure 12: Sensor Setup [11] ..... 27
Figure 13: Experiment Setup [12] ..... 27
Figure 14: FFT of Gesture Waveform ..... 29
Figure 15: EMG Active Segment[24] ..... 30
Figure 16: Filter Feature Selection Approach [39] ..... 34
Figure 17: Wrapper Feature Selection Approach [39] ..... 35
Figure 18: SAX Discretization [17] ..... 38
Figure 19: Log Likelihood / Probability Correspondence ..... 42
Figure 20: One-Against-All Approach to SVM Training [37] ..... 43
Figure 21: Confusion Matrix Example ..... 50
Figure 22: SVM Wrapper Threshold Calculation ..... 51
Figure 23: Signal to Noise Difference Threshold Calculation ..... 52
Figure 24: SVM Wrapper Number of Frames Calculation ..... 53
Figure 25: Filter Based Feature Ranking ..... 54
Figure 26: DTW 8 Class Confusion Matrix ..... 58
Figure 27: DTW 8 Class Precision and Recall ..... 58
Figure 28: DTW 18 Class Confusion Matrix ..... 59
Figure 29: DTW 18 Class Precision and Recall ..... 59

Figure 30: Gesture 2 Iteration Distances from Templates ..... 61
Figure 31: Example Misclassification Distances ..... 61
Figure 32: HMM States and Symbols Test ..... 63
Figure 33: HMM Number of Skipped States Test ..... 64
Figure 34: HMM Accuracy Over Number of Classes ..... 65
Figure 35: HMM Minimum Amount of Training Data ..... 66
Figure 36: HMM Recall and Precision Test ..... 67
Figure 37: HMM Optimized Results ..... 68
Figure 38: HMM Sub-Optimal Test ..... 68
Figure 39: HMM Gesture Separability ..... 68
Figure 40: Movement ID and Descriptions [12] ..... 69
Figure 41: SAX Discretization Confusion Matrix ..... 70
Figure 42: SAX Discretized Recall and Precision ..... 70
Figure 43: SAX Individual User Results (Overfitting) ..... 71
Figure 44: SAX General Test (Underfitting) ..... 72
Figure 45: Linear Kernel Average Cross Validation Ratio ..... 73
Figure 46: RBF Kernel Parameter Search ..... 74
Figure 47: SVM Performance vs. Number of Classes ..... 74
Figure 48: SVM Learning Curve ..... 75
Figure 49: SVM Optimized Average Cross Validation Ratio Results ..... 76
Figure 50: SVM Optimized Recall and Precision ..... 77
Figure 51: SVM Time Complexity ..... 80
Figure 52: HMM Time Complexity ..... 80
Figure 53: DTW Time Complexity ..... 80
Figure 54: Overall Classifier Performance ..... 81

# List of Tables

Table 1: HMM Wrapper Feature Subset Scores ..... 55
Table 2: SVM Wrapper Feature Subset Scores ..... 55
Table 3: SAX vs. Down Sampling DTW..... 57
Table 4: Ninapro Classification Results ..... 78

# Acronyms

| | |
|---|---|
| ACVR | Average Cross Validation Ratio |
| ANN | Artificial Neural Network |
| ANOVA | Analysis of Variance |
| APR | Average Precision Ratio |
| ARR | Average Recall Ratio |
| ASL | American Sign Language |
| DP | Dynamic Programming |
| DTW | Dynamic Time Warping |
| ECG | Electrocardiography |
| EMG | Electromyography |
| HMM | Hidden Markov Model |
| KNN | K-Nearest Neighbors |
| IMU | Inertial Measurement Unit |
| MAP | Muscle Action Potential |
| MN | Motor Neuron |
| MU | Motor Unit |
| MUAP | Motor Unit Action Potential |
| RBF | Radial Basis Function |
| SAX | Symbolic Aggregate Approximation |
| SFS | Sequential Forward Selection |
| SFFS | Sequential Forward Floating Selection |
| SVM | Support Vector Machine |

# 1 Introduction

## 1.1 Background Problem

There is a current trend in technology to expand the use of custom wearable devices. Such gadgets range from portable phones to smart watches and recently the onset of custom smart prosthetics. It is precisely the expansion of these technologies which has propelled forward the study of machine learning oriented activity recognition. In this context, machine learning is the use of computational tools to extract and decipher a pattern within data. The recognition of these patterns is then molded towards an end goal of use, such as recognizing a human action, and through it, a person's intent.

The work that follows tries to aid in the study of this field by making a comparison of the implementation and the optimization of different machine learning methods for gesture recognition. Though the end goal of gesture recognition and classification might seem better suited for a tool such as cameras, which would avoid the hindrance of having electronics attached to the body, this work begins with the assumption that alternative approaches to gesture recognition are not feasible in many situations. For instance, cameras require very structured environments to capture data in a way that could be used for a computer system and gesture recognition. Lighting becomes an issue, as does the possible use of such a system in spaces void of a proper camera setup. Instead, this work makes the assumption that there are many more benefits to a wearable device.

Such a device might eventually be used in multiple contexts where gesture recognition is an option. For instance, much research has gone into using such a system for sign language translation into speech and vice versa. This capacity would allow for better communication between people, and would be based on the already gesture defined American Sign Language dictionary shown in Figure 1. Another use of a gesture recognition system lies in swat team and military operations which often make the use of tactical hand signs. These signs, as shown in Figure 2, supplement speech where concealment is needed such as in tactical operations, or where high noise levels overpower the voice, such as landing zones. Finally, the last example which will be

offered also covers the principal motivation of this work, that of smart prosthetics for upper limb amputees.


Figure 1: ASL Hand Signs, J. Strickland, "The Sign Language Alphabet," *How Stuff Works*, 2007. [Online]. Available: http://people.howstuffworks.com/sign-language2.htm.
Used under fair use, 2014.

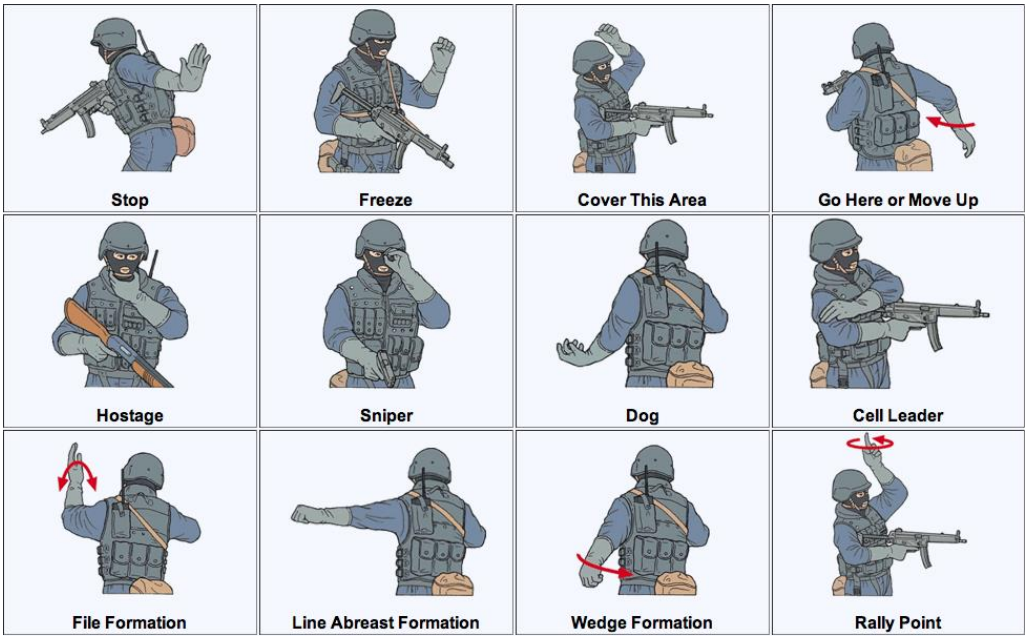


Figure 2: SWAT Team Hand Signs, S. A. R. Tidwell S. Karlaputi, R. Akl, K. Kavi and D. Struble, "Evaluating the feasibility of EMG and bend sensors for classifying hand gestures," in *Proceedings of the International Conference on Multimedia and Human Computer Interaction (MHCI-13)*, 2013.
Used under fair use, 2014.

In the USA, there are an estimated 50,000 new amputations every year [3]. Of those, roughly 10,000 are amputations of the upper extremities [4]. Though passive prosthetics have been the most popular option thus far, electromyography (EMG) controlled active replacements are quickly gaining traction in the medical community. This is due to the increased control and quality of life such an option offers.

After an amputation, forearm muscles remain largely intact [5]. Evidence even subjects that EMG signals from amputees are very similar to those generated by intact subjects [6]. For instance, even though intrinsic muscles, which control many degrees of freedom, are no longer present for below the elbow amputees, it is still possible to control certain degrees of freedom such as hand flexion and extension through extrinsic forearm muscles [7]. This is why the following work, like many such works in this field, makes the use of intact subjects which are more readily available for testing proof of concept trials. The methods which culminates from these tests can then be translated to amputees with little loss of functionality or generalization.

Using these assumptions and approach, multiple systems have been developed which seek to offer multi-functional prosthetic control. For example, Figure 3 shows a system overview of the work done by Dr. Marko Vuskovic which demonstrates the process many researchers seek for prosthetic control: EMG collection, feature extraction and classification, force and movement mapping, and finally control [8].

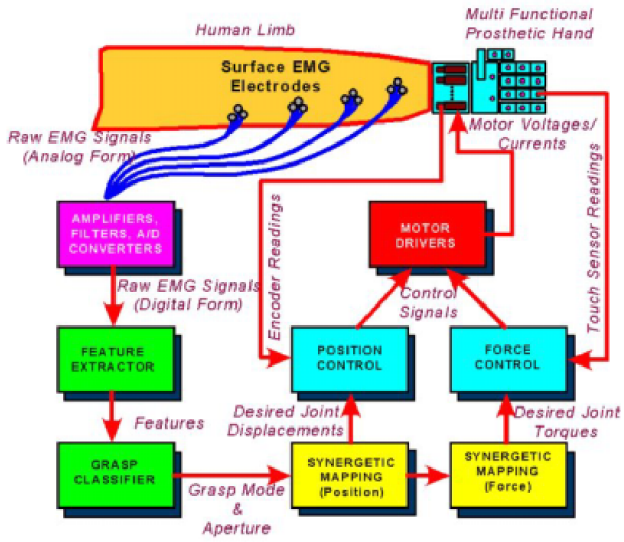


Figure 3: Control Strategy for Smart Prosthetics, A. Esquenazi, "Amputation rehabilitation and prosthetic restoration. From surgery to community reintegration," *Disabil. Rehabil.*, vol. 26, no. 14–15, pp. 831–836, Jan. 2004. Used under fair use, 2014.

## 1.2 Proposed Solution

Gesture recognition is an old problem with many proposed solutions. Even though the Holy Grail of gesture recognition is to simulate human vision and use passive systems, such as cameras, this technique suffers from major drawbacks. For instance, finger occlusion can be very high depending on point of view. Because of this issue, multiple gestures can look exactly the same to a passive camera [9]. Still many researchers have taken the vision based approach.

In this work, EMG based gesture recognition is proposed in order to alleviate some of the issues of vision based systems. With this technique, it is possible to avoid the point of view issue already mentioned, as well as other issues such as the required camera infrastructure, the necessity for a clear line of sight, any need for constant lighting, resolution and range problems, and even frame rate [10]. In order to do EMG gesture classification, this thesis compares three different machine learning tools, Hidden Markov Models, Support Vector Machines, and Dynamic Time Warping, to recognize different gestures classes. It further contrasts the applicability of these tools to noisy data in the form of the Ninapro dataset, a benchmarking tool put forth by a conglomerate of universities [11], [12]. Using this dataset as a basis, this work paves a path for the analysis required to optimize each of the three classifiers. Ultimately, care is taken to compare the three classifiers for their utility against noisy data, and a comparison is made against classification results put forth by other researchers in the field.

## 1.3 Thesis Structure

This thesis will deal with the design, analysis, and optimization of machine learning algorithms for use in gesture recognition. This work was motivated by the desire to apply machine learning tools to the improvement of machine human interface through electromyography. Such interfaces are quickly gaining traction in industry, with multiple recent startups gaining popularity [13]. Within this field, this thesis' achievements will concentrate on using such a system for smart prosthetics which might aid amputees.

As will be seen, much of this work deals with the optimization of multiple gesture classifiers through experimentation. There is also a large emphasis on the comparison of the methods chosen and how they might be suited for different kinds of data. Ultimately,

a choice is made based on repeated experiments on the classifiers and the EMG Ninapro database. Also, as will be seen, even though not a real time design, the accuracies achieved in this work are on par with current state of the art research systems, and could be extended to perform online recognition.

The rest of this thesis is structured as follows. Chapter 2 offers a variety of previous works in the field, specializing in gesture recognition for prosthetic control.

Chapter 3 will cover the background theory behind the major blocks of this work, beginning with electromyography, or the use of electrodes to measure muscle electrical potential; then upper limb physiology will be reviewed as it pertains to arm gesture recognition and prosthetic control. Finally, the three learning classifiers will be covered in order to give the reader a basic understanding of how they operate.

Following the background theory, chapter 4 will cover the methods used in this work in detail. This will include the datasets used for learning as well as the code used. Most importantly, chapter 4 also goes on to setup a number of experiments which were conducted in the search for classifier optimization.

Chapter 5 goes on to cover the results of the analysis. First, results for the data representation experiments are presented. These results show how the Ninapro dataset was represented for each of the three learning methods. Secondly, each of the three classifiers is studied in detail through their individual experiments.

Finally, chapter 6 will offer concluding remarks discussing the ultimate outcomes of the three gesture classifiers including their performance, the final achievements as the author sees them, and potential future work which might branch off from this thesis.

## 1.4 Summary

The current chapter has worked to setup the basic problem that this thesis tries to tackle. Through reading the background problem and proposed solution sections, the author hopes that the reader gets an appreciation for the realm this work fits into, and where it can be applied. Furthermore, this chapter has also worked to preview the remainder of this thesis and give the reader a roadmap for what is to come.

Now that the groundwork has been laid for the problem at hand, the following chapter will present a few of the numerous works available in the gesture recognition

community. Through these examples, the reader should get a sense of the diversity within this up and coming field, as well as where some of the ideas in this thesis come from.

# 2 Literature Review

## 2.1 Chapter Summary

Chapter 2 of this thesis will contribute two important aspects to setting up this work. First, it will concentrate on machine learning methods as they relate to gesture recognition. Second, certain works will be reviewed which although outside the scope of the current work, nonetheless show future development which might spin off from this work. On the first topic, while there are too many such works to cover them all, the following few have been chosen as those with the greatest effect on this work. In investigating these, the reader should get a sense of how popular and diverse machine learning gesture recognition is.

## 2.2 Previous Research

There are a lot of works which concentrate on wearable devices for gesture recognition. These works range in scope from small projects by undergraduate engineering students, to Master's Thesis, and much further into million dollar projects such as that conducted by NASA's JPL. What follows are a few such works that contributed to this thesis, either by offering simple guidelines, explanations and examples, or even aiding in defining the scope.

Of the works studied in preparation for this thesis, the work by Zhou et al. showed the most similarity to the methods followed here [14]. These researchers use a dense sampling of EMG signals, extracting information through a process similar to what will be detailed in chapter 4, even using some of the same features and feature selection approaches. There is however, one main difference of this work with what is proposed here; instead of using residual forearm muscles for EMG collection, Zhou et al. go a step further and assume complete loss of the limb, collecting sensor data from the pectoral muscles which they show also contain information about arm movement [14]. Examples of the type of approach followed by Zhou et al. will be further detailed in chapter 4 during the data preprocessing and feature extraction steps.

Much work has also gone into the developing and standardization of an EMG prosthetic system. Li of the Shenzhen Institute of Advance Technology is one such researcher [15]. In his work, Li follows the standard approach for EMG extraction and

preprocessing as will also be used in this work. However, he also goes on to propose a whole prosthetic control system based on a motion classifier, and a novel speed classifier based on specific EMG features, all of which revolve around the EMG amplitude. Results of this work show that patients gained the ability to control wrist – elbow, and hand movements with mean accuracies of 96% and 87% respectively. Results also show a motion completion time of 0.38 seconds, showing the responsiveness of the system [15].Though this work dealt in large part with the speed classifier, it also contained some aspects which were taken and applied here. For instance, it sparked the idea of whole system development, which pulled attention towards classification times and current state of the art classification results.

One of the latest developments in the field of robotic control through gesture recognition has been made by the researchers at NASA's Jet Propulsion Laboratory (JPL) [5]. There, a sleeve containing 16 dry contact EMG sensors has been used for various kinds of robot control. In this work, Wolf et al. broke robotic control into individual modes: Mimicked manipulation, Virtual joystick, stored procedure, and point-to goal [5]. They are also able to switch between command sets and even between different robots during operation. In this work, Wolf et al. also used SVMs to train $N(N-1)/2$ classifiers (where N is the number of gestures) for EMG and IMU classification. They used a feature space based solely on the individual signals' standard deviations over a series of windows to do both static and dynamic classification. With this method a 96.6% accuracy was achieved in a 17 static gesture set, and 99.8% accuracy in a 11 static gesture set; furthermore, a 99% correct classification rate was achieved in the dynamic gesture set [10]. It was from this work that both SVM and dry surface electrodes gained credibility for this author while researching past approaches.

Another work which influenced the approach in this work is that of Pylvänäinen [16]. This work which concentrated on HMM, used left to right continuous assumptions to study the effects of quantization and sampling rate on gesture recognition. By doing so, Pylvänäinen managed to find the minimum requirements for good recognition hover at 8 bits per channel and 35 Hz for accelerometers. These values produced a gesture accuracy of over 90% on a 10 class gesture set [16]. This analysis influenced the formation of a series of experiments in this thesis which will be covered in following chapters, covering

both the applicability of left to right models as well as the effect of quantization when dealing with HMMs.

More recently, there have also been multiple works which have expanded the idea of gesture recognition, both as to its uses and its approaches. Of these, Nick Gillian's dissertation work is of particular interest given that it demonstrated the validity of Dynamic Time Warping to EMG gesture recognition [17]. In this work, Gillian uses all three of the learning approaches also used in this work, furthermore, his was the first work which detailed an approach to the use of DTW, as well as the SAX quantization method which will be covered in chapter 4. Although the end goal of Gillian's work concentrate on gesture recognition specifically for music, it nonetheless heavily influenced a lot of the approaches used here. This effect can even be seen in the experimental structures of his and this papers.

Although Gillian and other researchers agree that DTW contains computational issues which seem to reduce its efficacy when compared to other stablished methods such as HMMs, there are other works which seem to disagree. For this reason, the DTW approach was followed here with an open mind, and with high hopes of being able to avoid the issues which have plagued other works. For instance, in 2009 Wollmer et al. proposed a multidimensional DTW approach for multimodal fusion of asynchronous data streams [18]. Such an approach is very inviting given that many datasets for gesture recognition, including the one used here, contain EMG data supplemented with IMUs, bend sensors, and even kinematic data, often sampled at different rates. Though the choice to use multimodal data was not used here, the idea of multidimensional DTW was. It, combined with methods used by Gillian and others, influenced the use and optimization of DTW during the experimental phase of this work, more on this will be seen in chapter 4.

Other researchers have concentrated not on learning procedures but rather the representation of EMG data, specializing in time and frequency domain features. Of these works, which are numerous and diverse, those of Tkach et al. and  Tubingen were studied in preparation for this thesis [19][20]. Tkach et al. concentrated on time domain features for EMG recognition, and especially the stability of these features to disturbances such as sensor location, fatigue, and intended effort, all factors which would affect EMG gesture

recognition. Through these results, these researchers demonstrate how some features are more susceptible to disturbances while others are more rugged and offer better consistency from trial to trial. Meanwhile, Tubingen structured his research not towards specific features, but rather the process through which feature selection can be accomplished from a set of possible features. This work together with Tkach's guided the formulation of a feature set and a feature selection approach later in this work.

As in some of the previous works, there were some aspects found during the literature review which did not make it into this iteration of the thesis. These are works which fall under 'Future Work' category and are at the same time examples of the types of approaches that go into the current state of the art systems. For instance, Chen et al. from the University of Science and Technology of China studied the improved performance of gesture recognition when training data is expanded to include wrist worn acceleration sensors [21]. Their methods include the analysis of 24 gesture classes through the use of two surface EMG sensors and two accelerometers. The accelerometers were placed in the back of the hand and wrist in order to extract hand and wrist motion. Through experimentation and the use of ANOVA hypothesis testing, Chen et al. showed that the addition of accelerometers to EMG data improved recognition by nearly 10% [21]. Such improvement although very inviting, are left for future works.

Singh et al., used a combination of wavelet packet transform and multi class SVMs to classify gestures for a six degree of freedom prosthesis [22]. Furthermore, by the addition of singular value decomposition for dimensionality reduction, they were able to achieve over 96% recognition rates. Their method consisted of identification through two EMG channels containing signals from the major forearm muscles. Ultimately, their work showed that singular value decomposition made a drastic improvement on recognition rates when using one-against-all SVM recognition [22].

Also, in contrast to standard methods like SVMs and HMMs, Liarokapis et al. used a method of inverse identification with random forests (which are made up of many decision trees) to identify individual movements [23]. In this model, they used kinematic measurements from a dataglove to feed a random forest which did the jobs of classification and identification of muscle activation for individual grasps. With this

approach, Liarokapis et al. found improved results when compared to other classical methods such as SVM and Artificial Neural Networks (ANN) [23].

And finally, Zhang et al, used a combination of EMG and accelerometers to classify gestures from forearm sensors [24]. In their work they also used decision tree classifiers, which included a HMM classifier as its last level. With this approach, they achieved gesture recognition accuracy in the range of 95%-100% [24].

As can be seen from this brief overview, the works in gesture recognition are broad and very distinct in their approaches. Many such works were studied and parts of them borrowed for this work. Also, as was already mentioned, possible future work following this thesis would further explore these works and seek to incorporate and test more of their approaches.

## 2.3 Summary

Chapter 2 has emphasized previous works which have helped form and guide prosthetic control. Through these few examples, the reader should get a sense that the machine learning field, as it is applied to gesture recognition, is ample and diverse, with much room for growth and experimentation.

These works and many more, were used in defining the methods which will be covered in the following chapter. These methods were the result of research into previous works combined with trial and error on the part of the author. With this in mind, the following chapter will begin to dissect the background theory necessary for understanding the approaches presented here.

# 3 Background Theory

## 3.1 Chapter Summary

This chapter will give a theoretical background on the major topics of this thesis. In so doing, it will cover EMG signals and their relation to the human forearm physiology, as well as machine learning techniques used to make sense and classify hand gestures for use with active prosthesis.

What follows is a brief background on the major topics of this work, beginning with EMG signals, their nature, and usefulness. Second, the physiology of the forearm will be investigated in relation to the independent muscles that might be of interest when it comes to gesture recognition. Finally, three machine learning tools will be described and presented in the context of gestures recognition.

## 3.2 Electromyography

Electrodes are commonly used in the medical community to measure muscle activation in relation to a patient's health. Electrodes do this by measuring the electrical activity of firing motor units (MU). An MU is made up of two parts, an alpha-moto neurons (α- MNs) which transmit commands from the central nervous system to a muscle, and the muscles which the α-MNs innervate [see Figure 4] [25].

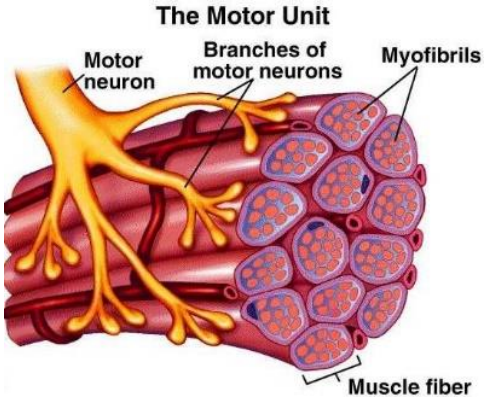


Figure 4: The Motor Unit, N. Shapiro, "Motor Unit Recruitment Strategies During Deep Muscle Pain," *The alchemist*. [Online]. Available: http://natchem.wordpress.com/2009/11/23/motor-unit-recruitment-strategies-during-deep-muscle-pain/.
Used under fair use, 2014.

Another important aspect of surface electrode, especially when compared to needle electrodes, is the fact that these sensor covers a finite area over a patient's skin.

The effect of this, which can be seen in Figure 5, collects a mixture of various motor unit action potentials (MUAPs) into a single sensor output.

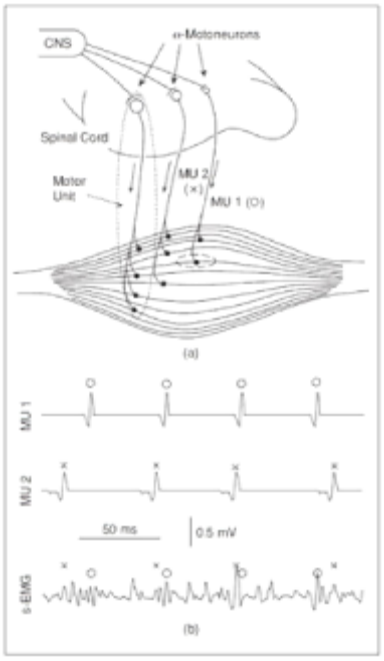


Figure 5: Motorneuron's EMG Signal Generation, G. A. Garcia, R. Okuno, and K. Azakawa, "A decomposition algorithm for surface electrode-array electromyogram," *Eng. Med. Biol. Mag. IEEE*, vol. 24, no. 4, pp. 63–72, 2005.
Used under fair use, 2014.

The combination of multiple MUAPs is called a Compound Muscle Action Potential (MAP); this is the signal captured by surface EMG sensors and lies in the range of 50µV – 30mV and 7-200 Hz [2] [4].

As useful as EMG signals may be, they are not without issues. Compared to other bio signals, EMG are susceptible to more types of noise that hinder proper signal processing. For instance, EMG signals are plagued by equipment noise, electromagnetic radiation from nearby sources, motion artifacts, in the range of 0 -15 Hz caused by the patient's movement, and even signal epenthesis as different MUAPs interact [27] [28]. The following are a number of other factors which can affect EMG signals and cause both issues as well as differentiate EMG on a per user basis [29]:

- Muscle anatomy which includes the number, size, and distribution of motor units.
- Muscle physiology which covers whether a specific muscle has undergone training, is affected by a disorder or is undergoing fatigue.
- Nerve factors such as nerve disorders.

- Contraction level resulting from the intended applied force from subject to subject.
- Artifacts such as the already mentioned movement artefact, or others such as muscle crosstalk and ECG interference.
- Recording noise from recording machinery, electrodes, and even testing location.

## 3.3 Physiology

In terms of gesture recognition, EMG sensors capture an array of signals from forearm muscles which correspond to different muscles associated with hand and wrist movement. These signals are a mixture of various muscles and their corresponding motor activations; although, machine learning (which we will look at more closely in following sections) can decipher the pattern in these signals as a background step for classification, it is still beneficial to try and understand how the muscle groups interact for specific movements before undertaking a gesture classification project. There are three main hand gesture activation methods and corresponding muscle groups [See Figure 6] we are concern with, these are [27] :

1. Finger flexion
    a. Flexor-digitorum-profundus
    b. Flexordigitorum-
    c. supercialis
    d. Flexor-polcis-longus
2. Finger Extension
    a. Extensor-digitorum
    b. Extensor-indicis
    c. Extensor-digiti-minimi
3. Thumb Extension
    a. Extensor-pollicis-longus
    b. Extensor-pollicis-brevis

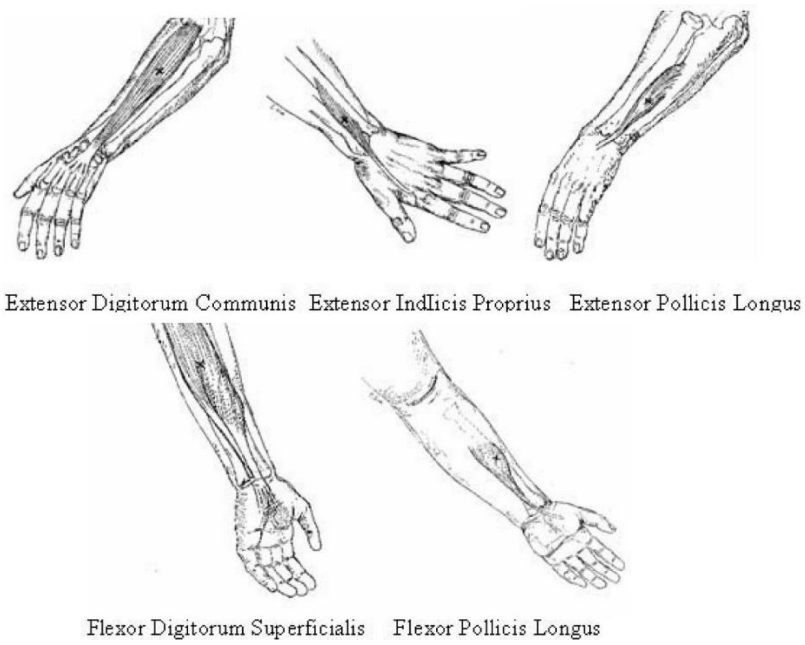


Figure 6: Forearm Muscle Groups, A. Zeghbib, *Forearm Surface EMG Signals Recognition and Muscoloskeletal System Dynamics Identification Using Intelligent Computational Methods*. 2007, p. 229.
Used under fair use, 2014.

As mentioned earlier, even though differentiating particular muscles groups is not necessary for the classifiers used here, an understanding of how each muscle interacts could be of tremendous use to some applications of this work. For instance, if the end goal is to design and control a robotic arm to mimic a human arm, then modeling the above muscles and their participation during particular movements could be of monumental importance.

## 3.4 Machine Learning

Machine learning is a tool which gives the ability for a computer algorithm to be trained with a dataset and solve a pattern matching problem. These techniques are able to detect patterns in data and apply these patterns to new problems in order to recognize or classify new occurrences.

An important consideration with machine learning techniques is the scope of the training data fed into the models. This decision has to be made early on as it will dictate the range of the model produced. For instance, training data from multiple users can be passed into the algorithm to produce a user independent model; or alternatively, data from a single user can be used to produce a model in a user dependent scheme. In the

case of EMG based gesture recognition, it has been found that individual gestures have high variances and standard deviations. This fact implies that each person performing the same gesture has their own unique gesture performing style [2]. Still, even though this seems to imply that a user dependent model is necessary, this work will test this assumption while also weighing the need for proper amounts of training data.

### *3.4.1 Hidden Markov Models*

Hidden Markov Models (HMM) are a well-known tool for sequence recognition. In the past they gained much popularity in the field of speech recognition due to their intrinsic temporal capacity. HMMs can estimate both the probability of an observation given a state, as well as the probability of an entire observation sequence occurring given a model [17]. Thus, given N number of models (one for each gesture), HMMs can give us the maximum likelihood of a gesture class taking place from a set of observations (EMG recordings).

There are certain important parameters to consider when working with HMMs. For instance, the models are created based on a feature space which has to be first extracted from the data. As such, the computational complexity of the HMM recognition is linearly dependent on the number of dimensions in the feature vector [16]; this means that care must be taken when discretizing the EMG recordings. It has also been found that for speech as well as gesture recognition, a left to right HMM offers the best accuracy [16]. A left to right model implies a system in which the model's states have to always move in an ascending pattern. This contrasts the alternative approach in which all the model's states are inter-connected [See Figure 7] [17]. This is an important consideration due to the computational complexity that comes from operating on a sparse vs. a dense matrix.

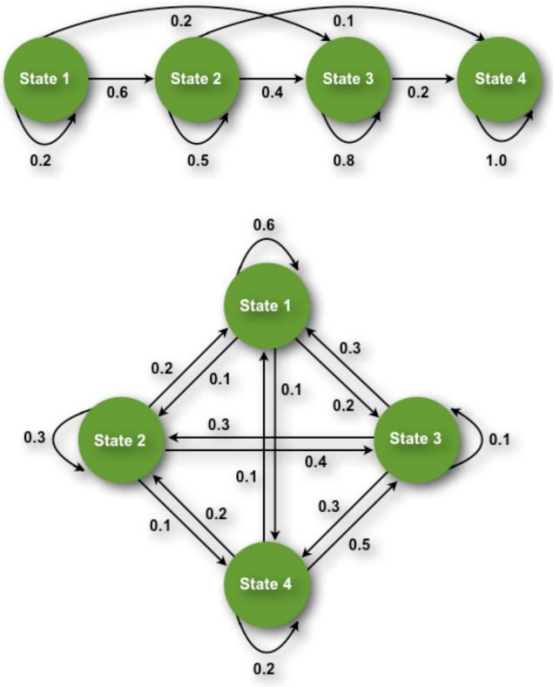


Figure 7: HMM Topologies, left to right (top) and ergodic (bottom), N. E. Gillian, "Gesture Recognition for Musician Computer Interaction," Queen's University Belfast, Ireland, 2011.
Used under fair use, 2014.

The basic idea behind HMM lies in being able to estimate the value of a hidden state given certain observations caused by that state. For example, imagine a recluse who has no contact with the outside world and hence no way to know of the weather, except for the small interaction with a friend who brings in the daily paper. Some days said friend brings an umbrella with him, other days he wears shorts and sunglasses, and yet others a large coat. For a few days upon arrival the friend also informs the man of the state of the weather outside. Given these observations and a few known outcomes it becomes possible for the man to begin making educated guesses about the current day's weather based solely on new observations of his companion's clothing. This simple example illustrates how a hidden state (the weather in this case) and a series of observations (daily garments) can be used to train a model and guide smart prediction making based on visible emissions. The assumption can also be made that the model's emissions will be either discrete (umbrella or no umbrella) or continuous (outcome of quantitative formulation).

Assuming discrete emissions, an alphabet can be formed which contains W number of possible emissions in hidden state set Z. And hence, Hidden Markov Models can be modeled by the following quantities [30]:

- Z: the number of discrete states in the model
- W: the number of discrete observation symbols per state
- Prior Probability $\pi$ : A vector with size (1 x Z) containing the probabilities of each state being in the starting state at time $t_0$

$$\pi_i = \Pr[X(t_0) = S_i], \quad i = 1, \ldots, Z$$

- Transition Probability A : Matrix with size (Z x Z) containing the probabilities of state $S_i$ at time $t_n$ transitioning to state $S_j$ at time $t_{n+1}$

$$a_{ij} = \Pr[X(t_{n+1}) = S_j | X(t_n) = S_i], \qquad i, j = 1, \ldots, Z$$

- Emission Probability B: Z x W matrix containing probabilities $b_{ij}$ of seeing emission $Z_j$ at time $t_n$ from state $S_i$.

$$b_{ij} = \Pr\left[Z(t_n) = Z_j \middle| X(t_n) = S_i\right]$$

$$where: b_{ij} \geq 0, \quad \sum_{j=1}^{W} b_{ij} = 1$$

- $\tau$: threshold value for rejecting null gestures (Optional)

The transition probability above is dependent on one constraint which forces all individual probabilities from any given state to sum up to 1. This means that a state must lead back to another in the set, or more generally that all states lead back to one another, and there are no states outside of the given set.

$$a_{ij} \geq 0, \quad \sum_{j=1}^{Z} a_{ij} = 1$$

Together, these quantities make up the HMM which is characterized by a prior, transition and emission probabilities, and rejection ratio.

$$\lambda = (\pi, A, B, \tau)$$

And thus a system wide HMM gesture recognizer is given by

$$\lambda = \{\lambda_1, \lambda_2, \ldots \lambda_N\}$$

Now that a base understanding of what a HMM is has been established, one can begin to understand what a HMM can do. There are three basic problems to solve when dealing with HMM:

1. Given a set of observations O, and a model $\lambda$, how is $P(O|\lambda)$, the probability of the observation sequence given the model, computed?
2. Given a set of observations O, and a model $\lambda$, how is a corresponding state sequence S computed which best explains the observations.
3. Given an observation sequence O, how can the model parameters be optimized to calculate the model $\lambda = (\pi, A, B, \tau)$.

For the problem of gesture recognition, problems 1 and 3 are the most important as they cover training the model (problem 3), and recognition (problem 1). These two problems can be solved by the Baum-Welch (training), and Forward-Backward (recognition) algorithms. Looking at the details of these algorithms is beyond the scope of this thesis; for more details of the specific mathematical relations please see Nick Gillian's dissertation on gesture recognition for music interfaces [17].

In the case of a gesture recognition system, each gesture model can be trained with multiple observation sequences for more robust recognition. This is done by calculating a model for each observation and combining them as:

$$P(O|\lambda) = \prod_{k=1}^{K} P\left(O^{(k)}\middle|\lambda\right) \text{ where K is the number of observations.}$$

Furthermore, a new observation sequence representing a gesture can be classified using the maximum probability of:

$$c = argmax_g \; P\left(O\middle|\lambda_g\right) \quad 1 \leq g \leq G$$

### *3.4.2 Dynamic Time Warping*

Dynamic time warping (DTW) is a template matching algorithm, which unlike likelihood-based tools like HMMs, does not require extensive training data. DTW measures the distance between input sequence and a class reference. What differentiates DTW from other template matching schemes is that it is able to deal with sequences of

different lengths. To do this the DTW algorithm performs a nonlinear distortion in the time axis, as shown in Figure 8, as to maximize the correlation between the two sequences.

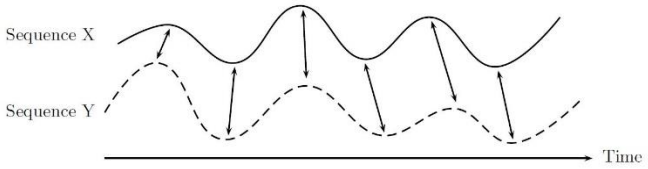


Figure 8: DTW Method, M. Müller, "Dynamic Time Warping," in *Information Retrieval for Music and Motion*, Springer Berlin Heidelberg, 2007, pp. 69–84.
Used under fair use, 2014.

In the past, this approach has been successfully used for speech recognition, due to its ability to deal with time dependent sequences. More generally, DTW can deal with feature sequences sampled at equal time intervals. The algorithm is also able to find an optimal 'warping path' $[p = (p_1, \dots, p_L)]$ between the two sequences of lengths N and M, which best transforms one input sequence into the reference frame of the template sequence. To do this the DTW algorithm must follow three rules:

1. Boundary condition: The warping path must start and end at the start and end of both sequences. That is, $p_1 = (1,1)\ and\ p_L = (N, M)$.
2. Monotonicity condition: warping path should always be increasing within the input sequences' indexes. $n_1 \leq n_2 \leq \cdots \leq n_L \leq \quad and\ m_1 \leq m_2 \leq \cdots \leq m_L$
3. Step size: warping path index should always increase by 1. Warping path should not move backwards.

Finding the optimal path is done through the use of dynamic programming (DP) and the calculation of a cost matrix. Using this approach a cost matrix can be calculated and the optimal path found by calculating the path with the minimum total cost; which is a user defined measure of similarity between points in the input sequences. Hence the total cost can be calculated as

$$c_p(X, Y) := \sum_{l=1}^{L} c\left(x_{n_l}, y_{m_l}\right)$$

Calculating the minimal cost from all possible warping paths could be done through brute force, by calculating the total cost of all possible warping path, and extracting the

minimum value. However, a better approach is through the use of dynamic programming. In this approach an accumulated cost matrix D is calculated which stores the warping cost values in a computationally efficient way. In fact, this approach reduces the cost of finding the optimal warping path from exponential complexity in N and M to a more manageable N*M complexity. The accumulated cost matrix D can be calculated through DP with the following formula:

$$D(n,m) = min\{D(n-1,m-1), D(n-1,m), D(n,m-1)\} + c(x_n, y_n)$$

By moving backwards from $p_L = (N,M)\ to\ p_1 = (1,1)$ through the lowest energy (also known as the valley) in the accumulated cost matrix D, the optimal warping path can be found [See Figure 9] [31].

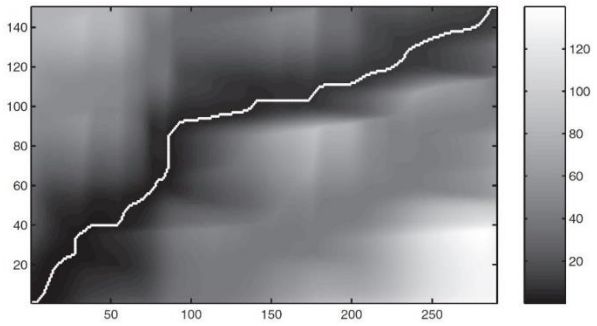


Figure 9: DTW Optimal Warping Path, M. Müller, "Dynamic Time Warping," in *Information Retrieval for Music and Motion*, Springer Berlin Heidelberg, 2007, pp. 69–84.
Used under fair use, 2014.

There are multiple variations of this technique. For instance, Holt et al. proposed a method of multi-dimensional DTW (MD-DTW) where the multi-dimensional series consists of measurements made at consecutive time intervals [31]. The specific dimensionality of this method consists on the number of measurements made. The algorithm presented by Holt is presented below on two series (A and B) containing K dimensions as an explanation of the steps required for multi-dimensional DTW

1. Normalize each dimension of A and B to zero mean and unit variance
2. Smooth dimensions with Gaussian filter if desired
3. Fill distance matrix D through:

$$D(i,k) = \sum_{k=1}^{K} |A(i,k) - B(j,k)|$$

4. Use distance matrix to find best synchronization path through standard DTW

Further adaptations can be made to MD-DTW, for instance dimensional reduction can be made. In this variation, individual dimensions on all series can be excluded if their variance shows them too contain too much noise, which might otherwise obstruct classification [31]. Additionally, much like with HMM, a variation can be made where a threshold value is added to reject null gestures. With this addition, the classification process through SVM becomes more akin to the process shown in Figure 10.

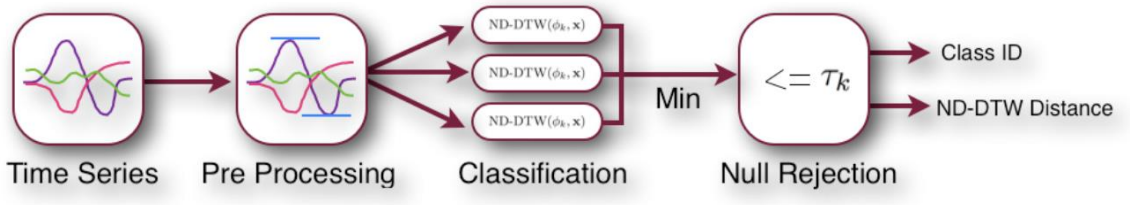


Figure 10: DTW Classification Process, N. E. Gillian, "Gesture Recognition for Musician Computer Interaction," Queen's University Belfast, Ireland, 2011.
Used under fair use, 2014.

Another important aspect of DTW gesture recognition is the calculation of the optimal gesture template for each gesture. These template will be what is compared against new incoming data series. The optimal gesture template can be found during training by taking the M training examples for gesture G and finding the optimal example which maximizes correct classification by minimizing the DTW distance. The mathematical calculation for the $gth$ template is as follows [17]:

$$Template_g = argmin_i \frac{1}{M_g - 1} \sum_{j=1}^{M_g} f(ind) * MD - DTW(X_i, X_j) \quad 1 \leq i \leq M_g$$

where $$f(ind) = \begin{cases} 1 & if\ i \neq j \\ 0 & otherwise \end{cases} \quad and$$

$$X_i, X_j\ are\ the\ ith\ and\ jth\ training\ examples\ for\ the\ gth\ gesture$$

At classification time, the correct gesture is calculated by finding the minimum warping distance between the incoming stream and the predefined gesture templates, and checking this decision against the gesture's classification threshold:

$$c = argmin_g \quad MD - DTW\left(Template_g, X\right) \quad 1 \leq g \leq G$$

$$\hat{c} = \begin{cases} c & if \quad d \leq \tau_g \\ 0 & otherwise \end{cases}$$

### *3.4.3 Support Vector Machine*

Support Vector Machines are a learning algorithm which utilize hyper plane boundaries to separate classes based on their feature representation. Although SVMs are binary classifiers, which in their most fundamental state find a line through a feature space R that separates two classes of data, they are able to expand to multi class classification problems [See Figure 11] [17]. For multi-dimensional expansion it is necessary to adopt a method known as 'one against all' classification. In this method k models are built, where k is the number of classes being classified. Each model is trained with a single class containing positive labels while all other classes contain negative labels [22].

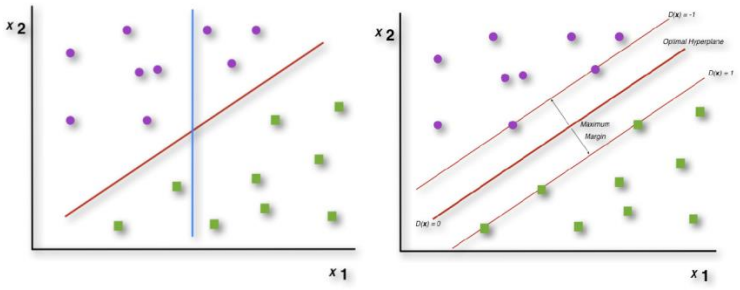


Figure 11: SVM Margin, N. E. Gillian, "Gesture Recognition for Musician Computer Interaction," Queen's University Belfast, Ireland, 2011.
Used under fair use, 2014.

For clarity, let's assume that the feature space to be classified is linearly separable. In this case a new gesture instance can be classified by training the SVM and observing which side of the division the new datum falls on. The calculations for classification are as follows:

$$D(x) = \sum_{i \in S} \alpha_i y_i w_i^T x + b_i$$

Where S is a set of support vectors, these are the vectors which form the division boundary, $w_i^T$ is the $ith$ support vector, $\alpha_i$ are a set of Lagrange multipliers that help unconstraint the problem, and b is a bias term given by:

$$b = \frac{1}{|S|}\sum_{i \in S}(y_i - w_i^T x_i)$$

Using this method a new feature vector, representing a new gesture, can be classified as:

$$c = \begin{cases} Class\ 1 & if\ D(x) > 0 \\ Class\ 2 & if\ D(x) < 0 \end{cases}$$

Though this method was originally presented as a linear classifier, it is able to classify non-linear/high dimensional data through the use of nonlinear kernel transforms. Using these methods, data is mapped into a higher dimensional feature space where a linear separation is possible. In this study two kernels will be tested. The first is the radial basis function kernel (RBF), which has been found to offer optimal results in gesture recognition [6]. This kernel is given by:

$$H(x, x') = \exp(-\gamma\left||x - x'|\right|^2)$$

where $\gamma$ is a positive parameter controlling the radius of the kernel. The second is the linear kernel given by the function:

$$H(x, x') = x^T * x'^T + c$$

The linear kernel is the simplest of all the kernel functions; in fact the use of the linear kernel is often equivalent to an algorithm's non-kernel counterpart. As seen in its formulation above, it is given by the inner product of $x$ and $x'$ plus an optional constant c [32].

## 3.5 Summary

Chapter 3 has covered the three mayor parts of this thesis. First, background on electromyography was covered, concentrating on how electrical signals are generated from motor units during movement and how these can be captured with the use of electrodes. Second, basic arm physiology was studied as it related to upper arm movements and gestures; here, an emphasis was put on those muscles which could be used for the design and control of a prosthetic arm. Finally, a large portion of this chapter went to the study of machine learning principles as they relate to gesture recognition. Within this section, Hidden Markov Models, Support Vector Machines, and Dynamic Time Warping were introduced alongside their basic parts and uses.

Using the knowledge gained from this and the previous chapters, the following chapter will setup the methods used in the current gesture recognition system design. This

chapter will be all inclusive, beginning with the chosen dataset, its preprocessing and extraction of feature data, the chosen representation of this data, and the application of each of the three learning methods to said data.

# 4 Methods

## 4.1 Chapter Summary

Chapter 4 will explore the methods used in conducting the experiments specific to this thesis. First, the dataset used will be covered in depth, including how it was collected, analyzed and segmented for use with the machine learning tools chosen. An in depth view of the features extracted will be given, and how they relate to both to the classifiers, and the gestures in the set. Following this, a series of experiments will be outlined which cover the rest of the system from feature selection to the optimization of each of the three individual classifiers.

## 4.2 Dataset

The decision was made to use an existing database for EMG data. The database goes under the name of "The Ninapro Project", it is a congregation of surface EMG and kinematic data from 27 intact subjects over 52 movements or gestures [11]. This database has been proposed recently as a benchmarking tool for hand prosthetics and gesture recognition. Hence, through its use, the results of this thesis can be compared to a larger body of work already available.

The data in the Ninapro database was collected using two separate tools. First, a 22-sensor dataglove (Cyberglove II) was used to measure kinematic data (finger positions). This glove represents joint angles as 8-bit values, which gives an average resolution of less than 1 degree. The Cyberglove is a standard device in virtual reality and clinical research. Secondly, surface EMG sensors were used to collect muscular activity; ten Deslys Trigno Wireless active double-differential electrodes (OttoBock MyoBock 13E200) were used. Using this system, EMG signals are synchronously sampled at 2 kHz; these sensors also include 3 axis accelerometers sampled at 148 Hz [12]. Ultimately, these sensors provide a signal that is amplified, bandpass-filtered, and rectified [11]. The electrodes are evenly spaced around the forearm just below the elbow at a fixed distance from the radiohumeral joint. Ten more sensors are placed on the flexor and extensor muscles [11]. The sensor locations can be seen in Figure 12, where 1 represents the equally placed electrodes, 2 are the spare electrodes, 3 corresponds to an inclinometer and 4 is the Cyberglove II, which includes its own 22 sensors.

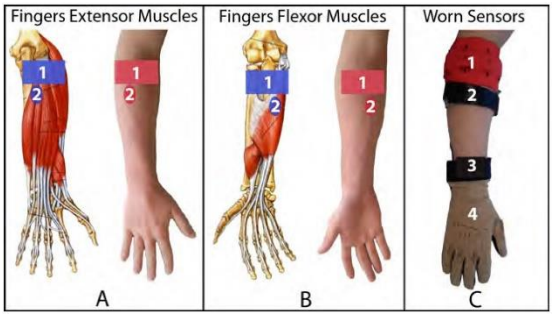


Figure 12: Sensor Setup, M. Atzori, A. Gijsberts, S. Heynen, A. M. Hager, O. Deriaz, P. van der Smagt, C. Castellini, B. Caputo, and H. Muller, "Building the Ninapro database: A resource for the biorobotics community," in *Biomedical Robotics and Biomechatronics (BioRob), 2012 4th IEEE RAS & EMBS International Conference on*, 2012, pp. 1258–1265.
Used under fair use, 2014.

A total of 52 movements were chosen from basic hand postures and grasps from the literature [for more info on the gestures, see appendix A]. These movements include:

- 12 movements of the fingers
- 8 hand postures
- 9 wrist movements
- 23 "functional" movements (grasping daily-life objects)

Using this set, the subjects were instructed to in turn replicate each gesture. To do this, they were comfortably seated in front of a screen which showed the gesture to be replicated. Each gesture lasts 5 seconds and 3 second are allowed for rest in between gestures in order to minimize the effect of muscle fatigue. The choice of hand is user dependent, and usually depends on the user's dominant hand. After a choice of arm was made, each sensor was applied to the skin as can be seen in Figure 13. In terms of using this data for classification, either hand is suitable given that multiple experiments have shown both hands generate extremely similar EMG waveforms [28].

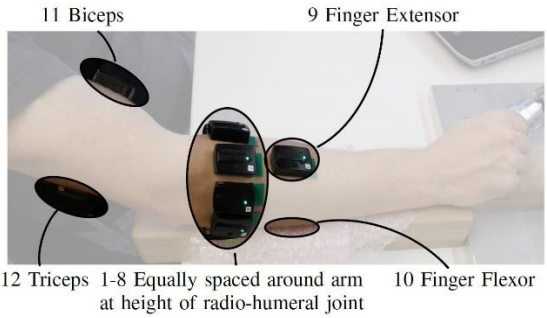


Figure 13: Experiment Setup, A. Gijsberts, M. Atzori, C. Castellini, H. Muller, and B. Caputo, "The Movement Error Rate for Evaluation of Machine Learning Methods for sEMG-based Hand Movement Classification," *Neural Syst. Rehabil. Eng. IEEE Trans.*, vol. PP, no. 99, p. 1, 2014.
Used under fair use, 2014.

Previously, it was concluded that EMG signals lie in the range of 7-200 Hz; taking this into consideration, the Ninapro dataset was sampled at 2000 Hz. This sampling frequency was based on the Nyquist-Shannon sampling theorem which states that sampling frequency must be at least twice as large as the largest frequency of interest. Too low a sampling frequency will not allow the tracking of fast changing signals. Aliasing can also become an issue with a low sampling frequency; this is a phenomenon in which frequencies become indistinguishable from each other in the sampled waveform. At the same time, too high a sampling frequency would alleviate these issues at the cost of high computation time. With high sampling rates come large number of samples per waveform. As the number of sensors and gestures increase, this can lead to unacceptable processing times. Hence, the Nyquist-Shannon theorem provides the minimal frequency to be able to capture the required signal bandwidth [27].

It was previously mentioned that this thesis deals with the recognition of gestures in the presence of noise. In fact, the idea that the data is plagued by noise issues becomes more and more important as the experimental results are presented in the following chapters. However, so far there has been no definition of how the noise issue presents itself, rather only a list of possible noise sources was presented in section 3.2. In order to illustrate and offer a quantitative measure of what noisy EMG signals might look like, the following analysis was conducted on multiple sample gestures using a FFT. As has already been stablished, EMG signal power is expected in the range of 7-200 Hz, hence strong signal content outside this range indicates noise that conceals the desired EMG data. As can be seen in the figure below, this is in fact the case with the data from the Ninapro dataset. Although most of the signal power lies in the expected range, there is also much content pass the 200 Hz limit. Furthermore, it is also difficult to separate the noise inside the expected frequency range, for instance that of movement artifacts (~15 Hz). Because this issue can be seen in all the signals within the dataset, the whole set is considered to be noisy and is thus treated as such. In future work, this same simple test can be used as a quantitative measure of EMG noise.

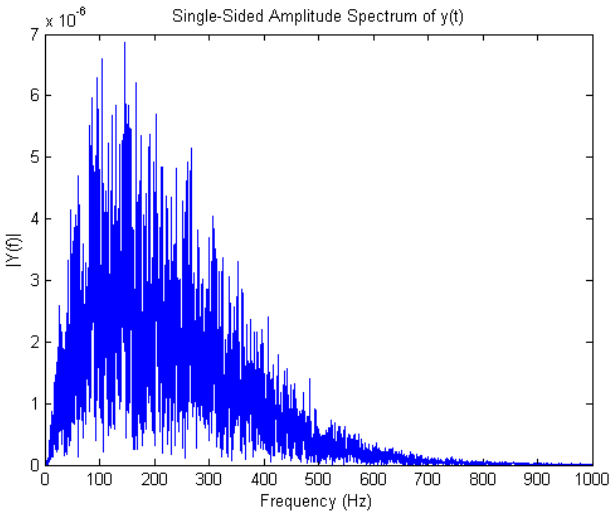


*Figure 14: FFT of Gesture Waveform*

## 4.3 Active Segments

The data from the Ninapro dataset has been used for gesture recognition. This process starts by selecting active segments, extracting a feature set from the data streams, and feeding the feature sets into the machine learning algorithms.

The first step in the software created for this work was to segment the data into a usable format. Because the data was sampled at different intervals, the accelerometer data is first up sampled to 2 kHz to match the EMG data [12]. Once this has been done, the dataset contains signals corresponding to a number of gestures and also synchronized in time. Hence it becomes possible to split each entry from the dataset into active segments containing the individual gestures performed. In between each gesture there is also a space of inactivity; this period could also be used to extract a 'null' gesture.

An active segment can be detected using a series of four steps on the raw EMG data [see Figure 15] [24].

1. Compute average of all EMG channels in use

$$EMG_{AVG}(t) = \sum_{C=1}^{N_C} EMG_C(t)$$

2. Apply moving average filter with a window size of W on the squared average EMG data.

$$Energy(t) = \frac{1}{W} \sum_{i=t-W+1}^{t} EMG^2{}_{avg}(i)$$

3. Detect active segments using two thresholds. The starting threshold is first used to identify the starting point of a gesture. This threshold should be high enough to prevent false positives. The ending threshold is to be used to locate the end point of an active segment. In contrast with the starting threshold, the end value should be low enough to prevent the unnecessary fragmentation of otherwise complete gestures.
4. Finally, those active segment whose length falls below a predetermine length, should be discarded. These segments are most likely not gestures but rather noise.

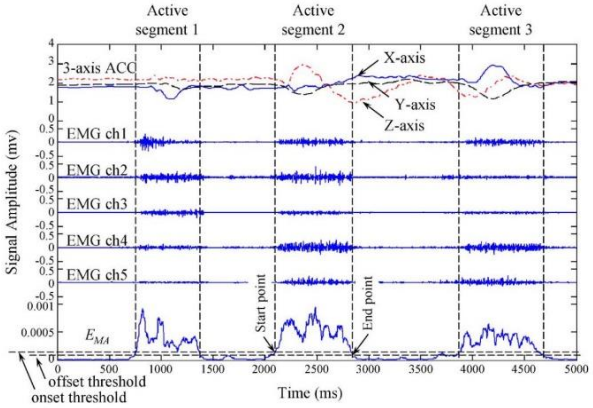


Figure 15: EMG Active Segments, Z. Xu, C. Xiang, L. Yun, V. Lantz, W. Kongqiao, Y. Jihai, X. Zhang, X. Chen, A. Member, Y. Li, K. Wang, and J. Yang, "A Framework for Hand Gesture Recognition Based on Accelerometer and EMG Sensors," *Syst. Man Cybern. Part A Syst. Humans, IEEE Trans.*, vol. 41, no. 6, pp. 1064–1076, 2011.
Used under fair use, 2014.

## 4.4 Feature Extraction

To begin analyzing the data using machine learning techniques, it is often necessary to convert the data into a feature space. Hidden Markov Models and Support Vector Machines are no exceptions. In this case, the active segments previously extracted, were further divided into individual blocks with length of 250ms, at every 125ms. This windowing technique utilizes a 50% overlap, and will be further explored during testing. It has been shown that an overlapping windowing technique results in

better performance than a disjointed one [33]. Furthermore, each channel within these windows is filtered by a Hamming window in order to remove unwanted effects from edge discontinuities [24]. The size of the window to test is often debated in EMG literature. The important aspects to remember are that the window size must be long enough to capture the temporal pattern in the signal, while at the same time being short enough to maintain the assumption of signal stationarity [34].

Some of the most popular and widely acknowledge features are listed below. They have been chosen for their ability to differentiate EMG signal based gestures. For instance, the standard deviation feature has been shown to be a good measure muscle activity, as it is well correlated to signal energy while remaining invariant to amplitude differences. Other commonly used features are number of zero crossings, slope sign change, and waveform length [10]. For a more detailed view into popular EMG features and their mathematical representation, please see appendix B [35].

1. Integrated EMG (IEMG): Calculated as the summation of the signal's absolute value. Often used as an active segment detector [36]

$$IEMG = \sum_{n=1}^{N} |x_n|$$

Where x is an EMG signal and N is the length of that signal

2. Mean Absolute Value (MAV): Estimate of the mean absolute value of signal. Frequently used to mark onset of a gesture [37]

$$MAV = \frac{1}{N}\sum_{n=1}^{N} |x_n|$$

3. Single Square Integral (SSI): Representation of the energy in the EMG signal [36]

$$SSI = \sum_{n=1}^{N} |x_n|^2$$

4. Variance of EMG (VAR): Estimate of the power content of signal. [7]

$$Sample\ Variance = \frac{1}{N-1}\sum_{n=1}^{N}(x_n - \bar{x})^2$$

Where $\bar{x}$ is the signal mean.

5. Root Mean Square (RMS): Estimate of standard deviation of signal. Also estimates power content of signal. [7]

$$RMS = \sqrt{\frac{1}{N-1}\sum_{n=1}^{N}(x_n - \bar{x})^2}$$

6. Waveform Length (WL): Cumulative length of signal. Contains information about signal frequency, amplitude, and duration. [7]

$$WL = \sum_{n=1}^{N}|x_{n+1} - x_n|$$

7. Willison Amplitude (WAMP): Measures motor unit activity while ignoring noise as defined by the threshold level. [7]

$$WAMP = \sum_{n=1}^{N} f|x_{n+1} - x_n| \ , \qquad f = \begin{cases} 1, & if\ x \geq threshold \\ 0, & otherwise \end{cases}$$

8. Log Detector (LOG): Provides an estimate of the force exerted by a muscle [35] [20]

$$LOG = e^{\frac{1}{N}\sum_{n=1}^{N} log|x_n|}$$

9. Slope Sign Change (SSC): Estimates frequency content of signal. Ignores noise as defined by threshold value. [7]

$$SSC = \sum_{n=2}^{N} f[(x_n - x_{n-1}) \times (x_n - x_{n+1})]$$

Where

$$f = \begin{cases} 1, & if\ x \geq threshold \\ 0, & otherwise \end{cases}$$

10. Zero Crossing (ZC): Estimates frequency content of signal. Ignores noise as defined by threshold value. [7]

$$ZC = \sum_{n=1}^{N-1}[sgn(x_n \times x_{n+1}) \cap |x_n - x_{n+1}| \geq threshold]$$

Where

$$f = \begin{cases} 1, & if\ x \geq threshold \\ 0, & otherwise \end{cases}$$

Extracting these features from the dataset was done with custom code based on the "Myoelectric Control Development Toolbox" put together by Chan et al. This toolbox is designed to allow researchers to have a common ground for comparison of EMG classifiers. The toolbox also contains other miscellaneous routines to facilitate filtering of raw EMG signals, as well as some tools for dimensionality reduction [38].

Three of the features extracted from the data require the previous calculation of a threshold value. This empirically found value is meant to facilitate the extraction of signal information whilst ignoring the effects of noise. In order to calculate the optimal value for this threshold, two tests were performed. The first is a process very similar to the feature selection wrapper method that will be explored in the feature selection section, while the second is a method based on the commonly used signal to noise ratio in signal processing.

For the first pass as the at threshold selection, the classification accuracy based on an SVM wrapper was used to test different threshold values. Using this method and averaging over many folds in k-fold cross validation, a consisted pattern could be extracted. However, the time complexity of this method quickly became apparent and diminished the ability to test a wide array of thresholds. To overcome the time constraints of the previous method, the second approach was utilized based on the signal to noise difference for each feature [7]. This method works by calculating a feature's average value during activity(S) and rest (N). Then, for a range of threshold values, the difference of signal(S) to noise (N) is calculated, with the highest S-N value giving the optimal threshold.

## 4.5 Feature Selection

In order to optimize classification accuracy, the extracted features were further reduced in number using feature selection methods. Ideally, every subset combination of features would be investigated and the optimum combination chosen. However, even with the thirteen features this work deals with, an exhaustive search such as this would

require more than 8,000 subset iterations. To alleviate this computational complexity problem, three feature selection methods are instead investigated. The first, consists of a simple filter method which can expand to all classification models. The second and third, Sequential Forward Selection (SFS) and Sequential Forward Floating Selection (SFFS) are wrapper based methods specific to an algorithm.

There has been much work done in feature performance for EMG gesture recognition. Multiple researchers have made use of tools such as sub-optimal branch and bound search, sequential forward-backward selection, Pudil's algorithm based on sequential forward backward floating search, and other variations of each of these. In these works, it has been widely accepted that SFS an SFFS are two of the best performing methods for feature selection; a fact that can be further accentuated by their widespread use over other approaches.

First, feature selection was approached using a distance filter method. These methods are based on specific filters which seek to quantify a feature's power at maximizing inter-class distance while minimizing intra-class distance. Using these quantities, filter feature selection then ranks tested features from most to least useful. Filter based methods are very popular in the literature due to their low level of complexity and value as a first indicator of feature importance. Nonetheless, due to the straight structure of this method, which can be seen in Figure 16, they are also to be used with care since no classifier information is fed back into feature selection.


Figure 16: Filter Feature Selection Approach, A. Shakoor, T. May, and N. Van Schijndel, "Soft computing based feature selection for environmental sound classification," Blekinge Institute of Technology, 2010. Used under fair use, 2014.

Two filters were tested for their discrimination capacity, the Fisher score and the Student's T-test. The Fisher score or Fisher Index, is a distance based metric which uses a feature's mean and variance per class (c) to compare and contrast the feature's power at discriminating between classes. The Fisher score is calculated through the following equation [40]:

$$\text{Fisher}(t) = \frac{\sum_{c_1,c_2}\left(\mu(c_1,t)-\mu(c_2,t)\right)^2}{\sum_c \frac{1}{|c|}\left(x(d,t)-\mu(c,t)\right)^2},$$
$$\text{where} \quad \mu(c,t) = \frac{1}{|c|}\sum_{d\in c} x(d,t).$$

The T-test method is a closely related metric which also makes use of a feature's per class mean and variance. Though in contrast to the Fisher score which works on a distance like metric, the t-test begins with the assumption that the two class means are identical. Through this assumption a p-value is calculated, and through the inverse of this value, the features in question can be ranked in order of most differentiable. It is defined as follows [41]:

$$Ttest(t) = \frac{\sum_{c1,c2}(\mu(c_1,t)-\mu(c_2,t))}{\sum_{c1,c2}\sqrt{\frac{\sigma_{c1}}{n_{c1}}+\frac{\sigma_{c2}}{n_{c2}}}}$$

Second, Sequential Forward Selection or SFS was conducted using both a SVM and an HMM wrapper. Wrapper based feature selection works to iteratively add (forward search) or subtract (backward search) from the feature subset available. Within this search, a 'wrapper' is the tool that is used to measure the feature subset's efficacy by feeding back information specific to a classifier. In this sense, the learning machine of choice, be it SVMs, HMMs, or other tools, are a black box to which we simply pass the selected features and from which we demand an accuracy [42]. This method of feeding back classifier data, as is shown in Figure 17, improves the performance of feature selection, though at the price of increasing the computational complexity of the method.

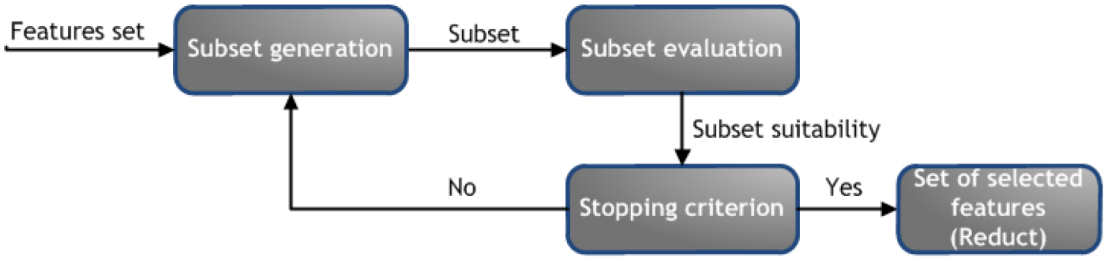


Figure 17: Wrapper Feature Selection Approach, A. Shakoor, T. May, and N. Van Schijndel, "Soft computing based feature selection for environmental sound classification," Blekinge Institute of Technology, 2010. Used under fair use, 2014.

SFS is a forward selection method, in that at every step it adds the feature with the most discriminatory value based on the wrapper's results. To do this, this algorithm starts

with a null subset of features and at every iteration adds and tests every feature not yet in the final subset through the chosen wrapper and records the average accuracy. It then picks and adds to the final subset, the feature with the best improvement. By doing this at every iteration the SFS algorithm ranks the best features and records their classification power. It then becomes up to the user to either place a limit on how many features to add to the final subset or at which classification accuracy to break the cycle [19].

Finally, the SFFS wrapper method was also used to automatically extract the optimum feature subset size. In this case a black box wrapper is also used; though the choice of stopping criterion is simplified for the user. This method works by combining the SFS method with a backwards step meant to simplify the model at every iteration. First, at the beginning of every iteration the method works just like the SFS method. Each feature not yet in the final subset is added and tested using the selected wrapper. The feature which offers the maximum improvement is then added to the subset list. At this point, instead of moving on to the next iteration step, like the SFS method, the SFFS method also incorporates a backwards step in which every feature is systematically removed from the subset. If the subset is found to improve by the removal of a feature, then that feature is permanently removed. By following these two steps at every iteration, the SFFS method improves on the performance of the SFS method in that the smallest and most powerful feature subset is chosen without the user having to indicate a number of features for the final subset [19].

## 4.6 Hidden Markov Models

Working with HMMs requires fine-tuning certain parameters to optimize classification. In the case of gesture recognition there are four main parameters this work investigated:

1. Number of states per model
2. Number of output symbols per model
3. Number of states that the model is allowed to skip over
4. Optimal feature representation

Additionally, two more tests were conducted to further compare the results and optimize the procedure.

5. Discriminatory power for different numbers of classes
6. Minimum number of training observations

### *4.6.1 Vector Discretization*

Because of the choice to use discrete Hidden Markov Models, as opposed to their continuous counterparts, it is necessary to discretize all observation sequences before completing any of the desired tests. In order to do this, the feature vectors which result from feature extraction must be clustered and separated into a number of discrete clusters. The k-means clustering method is used in this approach in order to divide the set of n training observation into the desired number of clusters [43]. Next, testing observations must also be split into these clusters at test time. In order to do this, there are two main methods available in the literature: the k-nearest neighbor approach and the closest cluster center approach [17] [44].

K-nearest neighbor (KNN) is a method through which a new observation is placed in the training feature space and its k-nearest neighbors are studied. These neighbors are checked for their cluster membership, and the most common membership is applied to the new datum [45]. In contrast, the closest cluster method makes use of the previously calculated training cluster centers. A new datum is awarded a cluster membership by placing it in the training feature space and finding the closest (usually in Euclidian distance) cluster center to it.

Still, other researchers argue towards refraining from the use of extracted features and k-means for clustering; arguing that EMG data is already soundly setup for discretization based on the SAX vector quantization approach [17]. SAX or Symbolic Aggregate Approximation is a method that alleviates noise issues inherent to k-means. Furthermore, if desirable SAX quantized data can be further quantized using k-means.

SAX is a process through which a single dimensional time series $x = x_1, x_2, \dots, x_L$ , of length L is able to be discretized to a secondary series $\hat{x} = x_1, x_2, \dots, x_S$, of length S, where S < L. The new series contains discrete values within a predefined and finite range [See Figure 18] [17]. In the case where the desired raw input is multi-dimensional, the SAX algorithm is applied to every dimension separately. Below are the steps taken for proper SAX discretization:

1. The raw series is first normalized to zero mean and unit variance
2. Time series is segmented into $f$ frames. The size (number of data points in window) of each frame is given by $\frac{L}{f}$
3. Mean value of each frame is calculated. This will be the value that is discretized using the alphabet.
4. Assign a discrete alphabet value to each frame following the following rule

$$\hat{x}_i = a_j \quad if \quad \psi_{j-1} \leq \bar{x}_i < \psi_j$$

here, $\bar{x}_i$ is the mean value of the ith frame and $\psi$ is a vector containing the break points for the predefined alphabet. These breakpoints are set such that the area under a Gaussian distribution of $N(0,1)$ from $\psi_{j-1}\ to\ \psi_j$ will be equal $\frac{1}{a}$.

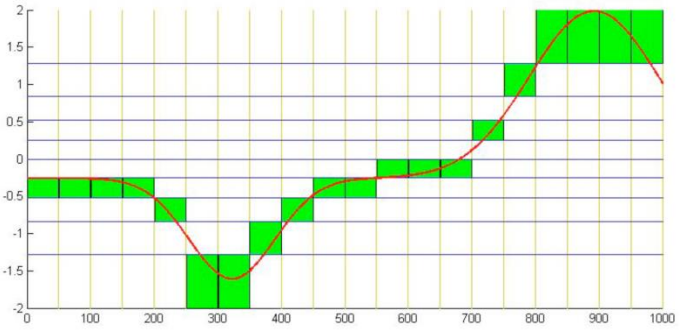


Figure 18: SAX Discretization, N. E. Gillian, "Gesture Recognition for Musician Computer Interaction," Queen's University Belfast, Ireland, 2011.
Used under fair use, 2014.

### *4.6.2 Model Setup*

As discussed in the HMM theory section, states in a HMM are not accessible. In fact, states are completely hidden from the user, and only recognizable through the emissions (symbols) they produce. In EMG gesture recognition, states can be thought of as the muscle interactions which occur when a movement is performed. These interactions take a number of forms (or states) which are impossible to see, were it not for EMG recordings (or emission symbols).

Training an HMM thus requires an estimation of the number of hidden states present in the real world phenomenon, as well as the number of emissions each state is viable to produce. In order to gauge the number of states and the number of emissions necessary for gesture recognition, $Nxk$ (where $N = 81, and\ k\ =\ 5$) models were trained using a k-fold training method. Each model followed a left-to-right approach, allowing for a single state to be skipped; each model was also constructed using a nearest cluster discretization method. For each model an average accuracy was calculated for all folds. By using a grid search over the number of state and symbols, with states and symbol ranging from 9 to 27, it was possible to estimate the optimal values for the final optimized models.

### *4.6.3 Left to Right vs. Ergodic Models*

Even though previous works in gesture and speech recognition have concluded that a left to right model structure is preferable over an ergodic structure, there have also been works which speak to the flexibility of each structure [17]. As seen previously, a left to right structure limits the model from skipping over states during the training phase. However, strictly enforcing that states have to be sequential might make the model too rigid for proper generalization.

In order to test this, a series of models were created using a k-fold training method (where $k = 5$). Each model iteration allowed an integer number of skipped states, ranging from 3 to 15. At each iteration, the models' accuracy were averaged over all folds.

### *4.6.4 Effect of Increasing Vocabulary*

Depending on the application for which gesture recognition is being applied, a different number of gestures or classes, are to be needed. For instance, if the task is to design a simple sign language translator, then a gesture recognition system needs around 26 recognizable classes. If the task is to recognize military hand signals, then a smaller number would be required.

The number of classes is important to keep in mind considering that detrimental effect that a large number of classes can have on recognition and classification. A large number of classes makes the classification problem more difficult and reduces accuracy

rates. Thus, when designing a new system, it becomes important to study the maximum number of classes that the system is capable of handling under acceptable classification results. To test for this number, a separate test was conducted which calculated the average cross validation ratio using 10 fold cross validation while varying the number of classes being tested.

### *4.6.5 Minimum Required Training Data*

Another important parameter of a gesture recognition system is the number of training instances that are required for optimal results. This parameter, unlike other parameters being studied, has an effect not only on the eventual results of the system, but also on the ease of setup. Even if the system resulted in near perfect classification accuracy, long setup times could prove harmful to the user experience and even deter possible users from the system. On the other hand, if the system requires little training data, then it becomes much more transparent and inviting to wide use by the public.

In the case of the current system, a number of tests were completed to identify the necessary number of training examples. From these tests, an optimal number of training iterations was identified which maximized accuracy while at the same time minimizing computation time.

### *4.6.6 Optimized Model*

Finally, a final test was conducted with the previously identified parameters which optimize gesture identification. Two variations of this test were performed to test out a final optimization technique. This last parameter has been the source of debate in the gesture recognition community. It is the difference between using a null gesture model as is often done in speech recognition with silence models [17] or using a validation threshold for rejecting null sequences.

While the two approaches differ drastically in their setup and implementation, they work toward the same end. In both cases, the goal is to recognize when a gesture is not being performed. For instance, if a subject is simply swinging an arm during a walking motion, this “gesture” should not be classified as some intentional movement. Some works have tried to resolve the issue of the null gesture by incorporating a trigger key into their systems [17]. Using this approach, an end user of the system, would have

an additional binary input signaling ‘true’ when a gesture is being performed and ‘false’ when no intentional gesture is underway.

Although the trigger key approach is very robust, it is not a natural solution. A hand gesture classifier should not force the user to add any motion to the natural flow of the movement. Thus, both the tested solutions would provide improved user experienced where no additional inputs are required, and instead the system itself decides when the ‘true’ and ‘false’ flags should be set.

The first solution tested consisted of adding a gesture class to the set that took the form of a null gesture. In order to do this, the non-active segments from the active segment extraction step were taken and compiled into their own null class. Then, a null gesture is simply treated as its own gesture and classified accordingly, with the only exception that the resulting act to this classification is no output. The null gesture can also be extended to encompass more than solely rest time. By adding a swinging arm motion, a scratching motion, or other inconsequential and aimlessly movements to this class, the null gesture can be extended to ignore unwanted movements.

On the other hand, the second solution tested for this issue takes the form of a validation threshold which must be applied when classifying a new gesture class. Much like the null gesture approach, this threshold is intended to differentiate between intended movements and a null gesture whose noise could be confused as a predefined class.

The use of this method adds one additional step to the recognition process, where a classified class is instead converted to a null class if its likelihood of belonging falls below a predetermined value.

$$\hat{c} = \begin{cases} c & if \quad P(O|\lambda_g) \geq \tau_g \\ 0 & otherwise \end{cases}$$

The classification threshold for each model can be calculated from the average of each trained model for each observation. A sensitivity margin is also added to allow the user to fine tune the number of standard deviations that will be acceptable for real-time prediction. The process for threshold calculation is given by [17]:

$$\tau_g = \mu_g - (\sigma_g \gamma)$$

*where*

$$\mu_g = \frac{1}{K_g}\sum_{i=1}^{K_g} P\left(O^{(i)}|\lambda_g\right)$$

*where $K_g$ is the number of observations in the gth gesture and*

$$\sigma_g = \sqrt{\frac{1}{K_g - 1}\sum_{i=1}^{K_g}\left(P\left(O^{(i)}|\lambda_g\right) - \mu_g\right)^2}$$

The above process calls for the probability of an observation given a gesture model. Because HMMs work in a log likelihood space, that probability will instead be replaced by the log likelihood that an observation belongs to the given model. Figure 19 below shows the relation between the two quantities and furthermore makes a good case for using the log likelihood as a way to avoid extreme values in the probability space.

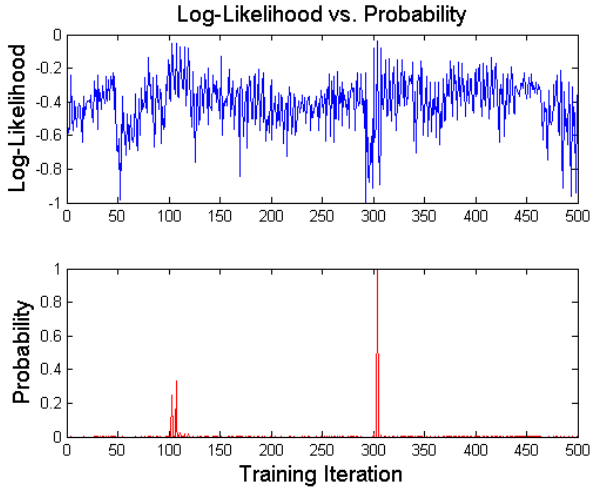


*Figure 19: Log Likelihood / Probability Correspondence*

The procedure detailed above has been shown to work well in some instances, however, the ideal solution for a hand gesture classifier is still the subject of debate and often differs on a case per case basis.

## 4.7 Support Vector Machines

LIBSVM was used as the based library for all the SVM tests. It is a library developed at the National Taiwan University. It is capable of support vector classification, both in two class and multiclass problems. The MATLAB wrapper for

LIBSVM was used in this work, through it, SVM classification is broken up into two steps: training and prediction. First, training data is used to train a number of models (one for each class). Then, these models are used to predict the probability that a new instance falls under each individual class. The class with the greatest likelihood of ownership is chosen as the class of the new datum.

Because SVMs are inherently binary classifiers, training new data is done through a one against all approach. In practice this means that at training time for each class, data from all classes is used, with data from the current class in question being given a value of 1, while all other classes are given a value of 0. Thus, the method of SVM training which is shown in Figure 20, means training a number of binary classifiers [46]. This method is commonly known as the one-against-all approach, and is perhaps the earliest and simplest implementation of multiclass SVMs [47].

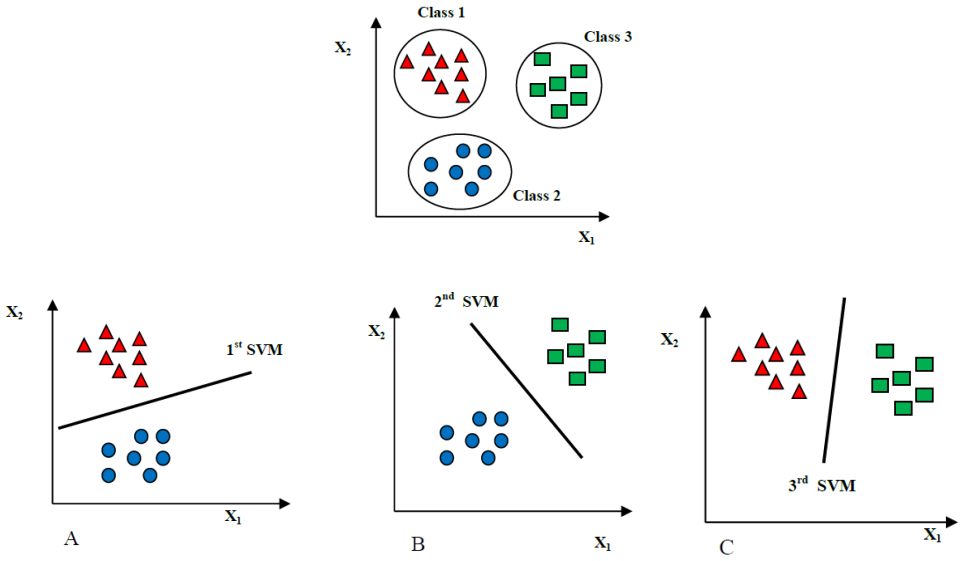


Figure 20: One-Against-All Approach to SVM Training, A. Hussein Ali, "An Investigation of Electromyographic (EMG) Control of Dextrous Hand Prostheses for Transradian Amputees," Ieee, 2013. Used under fair use, 2014.

### *4.7.1 Data Scaling*

For support vector machines it is necessary to scale the training data to be within a specified range, be it [-1,1] or [0,1]. This is due to the fact that otherwise each feature in the kernel space can have drastically different values, and some dimensions can overpower and drown out others. Also, because SVMs work on the inner product of feature vectors, improper scaling can cause numerical difficulties during processing. By

scaling each dimension to the same range, these problems can be avoided while ensuring that all dimensions are weighted equally.

Care must also be taken to properly scale the data during model generation. That is to say that testing and training data must be scaled in the same manner. This can also be viewed from the fact that no prior knowledge can be assumed form the testing data. Thus, the same scaling factors used in the training data must also be used for testing data. For instance, assume that a training feature with a range of [-100, +100] is to be scaled to [-1, +1], then if the same feature during testing lies in the range of [-150,+50], it must be scaled to [-1.5,+0.5] [48].

### *4.7.2 Kernel Test*

In order to optimize the required SVM parameters, a grid search was conducted using a 10 fold cross validation approach for each grid point. Both the linear and RBF kernels were tested for classification accuracy, with the linear variant serving as a comparison step for the more robust and popular RBF kernel. The C and gamma parameters were varied during in each step as powers of two (for a remainder of what these terms are, please refer back to chapter 3)[34]. From this search both the most powerful kernel and its most robust parameters were then extracted for use in the final SVM classifier.

### *4.7.3 Effect of Increasing Vocabulary*

As was already reviewed with HMM classifiers, there is a need to study the power of a classifier to a number of different classes. This means studying how the performance of classification decreases with an increasing number of classes to distinguish. In order to quantify these changes, a test was conducted which varied the number of classes to identify from 4 to 18. This test was conducted using the best performing kernel from the previous experiment, 10 fold cross validation, and a large enough number of training samples for proper training.

### *4.7.4 Minimum Required Training Data*

The last test necessary before a final method can be put together, is the calculation of the required amount of training data for proper training. The corresponding test was

conducted using a 10 fold cross validation approach for training, as well as being tested with both the linear and RBF kernels. At each run, a constant number of testing samples was extracted from the available data in order to minimize any bias which might be introduced by varying the number of testing samples.

### *4.7.5 Optimized Model*

Once the previous results were consolidated, a final test was conducted for overall classification accuracy. These test results served as the basis for calculating the average classification ratio, as well as the overall precision and recall. This test was also used as a time trial for comparison against the HMM classifier. One aspect that was not included in this test, was the comparison between the EMG defined null gesture vs. the threshold nullifying method. This is because, unlike with the HMM classifier, there isn't a good metric for determining a class instance's distance from the model. Instead, the EMG defined null gesture was used as part of the given class set.

## 4.8 Dynamic Time Warping

The first step in the process of utilizing the DTW approach consists of the preparation of the data into a form feasible for the computational complexity that results from a method involving constant grid searches. Alongside data representation, a useful number of training examples or iterations must also be finalized. Too many class example sequences would result in training times that are too long for proper use; on the other hand, too few class examples might not capture the cleanest version of each class. Arriving at a proper number of training examples requires some empirical data. It is also a value very dependent on the amount of computation power and time available. For this work, 15 iterations were chosen. Any more than this, and the method required too much processing time for it to be useful.

As has already been seen, implementing DTW in a multiclass classification setting involves the repeated use of the DTW method over a number of sequences. First, a number of iteration examples is collected for each gesture class and preprocessed. Second, these example sequences must be compared against each other in order to calculate the template gesture. As reviewed in section 3.4.2, the class template is found by finding the sequence that minimizes the iteration distance for every gesture. This is

done by comparing each example sequence for a gesture against every other sequence for that class and collecting the resulting DTW distances. The iteration that results in the minimum overall distance is then chosen to represent the class. Another description of this method might be to think of the template that is chosen as the most general of the example set. Because it shares the most with its fellow class members, the template can be considered the iteration with the least amount of noise, and the one which represents the motion in the way in which it was intended. As a side note of this part of the process, while a template is being calculated, the values for the overall distance can also be recorded alongside each individual distance between the template and its fellow class members. These distances are then used for to find the mean and the standard deviation of the distance data. The use of these two statistics will be seen shortly.

### *4.8.1 Data Preparation*

Two methods were tested for data preprocessing. The first consists of both down sampling and low pass filtering the raw data Through this method the sampling rate of a sequence of data is effectively truncated without adding any aliasing issues to the data [17]. The second method makes the use of the SAX algorithm, the details of which were covered in section 4.6.1. As a reminder, the SAX method consists of a way to down sample data through the grouping of similar terms in both time and amplitude. In both these approaches the amount of down sampling can be fine-tuned either by choosing a down sampling factor, or by hardcoding a set number of frames and amplitude range for a sequence.

### *4.8.2 Threshold calculation*

As with HMM, the classification threshold can be computed at the time of training with the use of training examples. The threshold value is intended to remove any classifications which fall below the training standard. In order to do this, a threshold is calculated at post processing time with the mean and standard deviation data collected during training time. The threshold is calculated as follows:

$$\tau_g = \mu_g + (\sigma_g \gamma)$$

Where $\gamma$ is a user defined number of standard deviations suitable for classification. The mean and standard deviations for each training example are calculated through the

following equation, which follow the standard definitions for mean and standard deviation for a waveform.

$$\mu_g = \frac{1}{M_g - 1}\sum_{j=1}^{M_g} f(ind) * MD - DTW\left(Template_g, X_j\right)$$

$$where\ M_g\ is\ the\ number\ of\ observations\ in\ the\ gth\ gesture$$

$$\sigma_g = \sqrt{\frac{1}{M_g - 2}\sum_{i=1}^{K_g} f(ind) * \left(MD - DTW\left(Template_g, X_i\right) - \mu_g\right)^2}$$

$$where \qquad f(ind) = \begin{cases} 1 & if\ i \neq index\ of\ template \\ 0 & otherwise \end{cases}$$

Once the threshold values have been calculated for each gesture class, they are stored for use at post processing time, where a classification might be nullified due to a distance value exceeding that of the threshold. The threshold value can also be updated continuously as more class members are added to taken away. Thresholds, like whole classes in this method, can also be trained independently of each other, allowing for parallel training which allows for a considerable shorter training times.

### *4.8.3 Optimized Model*

After the number of class members were settled and the data preprocessing method chosen, it was then be possible to compute a final classification test for overall accuracy. These results were compared before and after the use of the threshold value. As with the HMM method, the threshold approach was also compared to the null gesture implemented using the non-active EMG segments. However, because of the time complexity of DTW training, the starting assumption was that the use of the threshold nullifying method should be preferred over the EMG specified null class, as reducing the class set by one would improve training time.

## 4.9 Summary

This chapter has gone through the methods used in this thesis. In doing so, it has built on previous chapters by elaborating on the proposed solution described in chapter 1, borrowing certain tools from other works in chapter 2, and using the basic knowledge of

chapter 3. More importantly this chapter has also covered important implementation details, such as feature formulations, and libraries uses for machine learning. This chapter is one of the most important, given that it covers all the aspects that this author thought important when designing a new gesture recognition system. The experiments which have been laid out in this chapter will now be further studied in the following chapter alongside their results and the optimized models which spring forth for each of the three learning methods.

# 5 Results

## 5.1 Chapter Summary

Chapter 5 of this work presents the results achieved through the experiments described in the previous chapter. It begins with studies done on feature selection and representation, and goes on to test results for each of the three classifiers: DTW, HMMs, and SVMs.

In order to contrast the three learning approaches it is necessary to stablish a standard set of parameters that can be calculated across experiments and are representative of the overall results of each. As such, three classification errors were used from the work by Gillian, to evaluate the classification and recognition rates for each algorithm [17]:

- Average Cross Validation Ratio: classifier performance across all participants

$$ACVR = \frac{1}{K}\sum_{k=1}^{K}\frac{Number\ of\ correctly\ classified\ gestures\ in\ fold\ k}{Total\ number\ of\ gestures\ in\ fold\ k}$$

- Average Precision Ratio: Performance of exactness of classifier for each gesture over all participants

$$APR_i = \frac{Number\ of\ instances\ correctly\ classified\ for\ gesture\ i}{Number\ of\ instances\ classified\ as\ gesture\ i}$$

- Average Recall Ratio: Performance of classifier over specific gesture for all participants

$$ARR_i = \frac{Number\ of\ instances\ correctly\ classified\ for\ gesture\ i}{Total\ number\ of\ instances\ from\ gesture\ i}$$

In all of these formulas, K is the number of cross validation folds.

Another tool which will be used to evaluate each classifier's performance, is the popularly used confusion matrix. This tool is often used to visually assess a classifier's performance since it quickly demonstrates correct and incorrect classifications on a per class basis. Below is an example of a confusion matrix, the basic idea is to count the number of outcome classifications per class on the 'Output' axis (x-axis) against the correct classification on the 'Input' axis (y-axis). By doing this, a perfect classifier would have 100% classification count on the main diagonal, and 0% everywhere else. Instead,

what often happens is that incorrect classifications pop up outside the main diagonal, this effect can be seen in the figure as well. In order to make this visually easier, the values have also been color coded. This color code, which has also been applied to other results in this chapter, follows a basic heat map approach, where blues represent low values, and yellows and reds represent higher values.

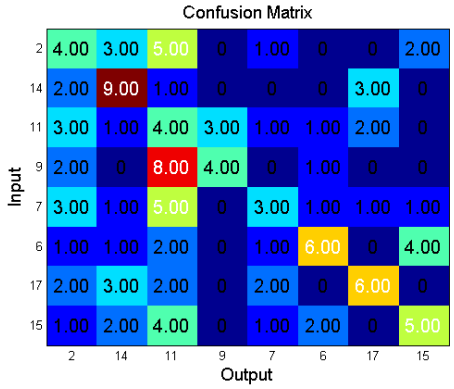


*Figure 21: Confusion Matrix Example*

## 5.2 Optimal Data and Feature Representation

One of the first steps in the process of finding the optimal classification system is to find the ideal data representation to use. It is not enough to simply extract the active segments which represent a gesture and pass the raw data to a classifier, instead the data must be transformed into a representation of itself which pairs most favorably with the classifier.

In the case of EMG signals where noise is a large concern, the data must be converted into a form where that noise is minimized. Some of the work to minimize noise was done at the active segment extraction step, however, some noise still remained within the active segments, which had to be considered. Additionally, the different time and frequency domain features that were used lend themselves to long computation and training times, thus feature selection must also be undertaken if a reliable system is to be design.

### *5.2.1 Feature Threshold*

The first series of tests conducted had the goal of minimizing noise within the extracted features through the use of a predefined threshold value. As covered in previous

sections, the noise in question is the result of diffusion though tissue, subject movement, suboptimal amplifiers, and other parameters often inherent to data collection.

To optimize the threshold, two tests were used. The first method borrows an idea from feature selection methods; that of a wrapper which can be used to test for a classifier's rate of accuracy .The wrapper used here is a 10-fold cross validated SVM classifier, which calculated the average accuracy over a range of thresholds. As can be seen in Figure 22, the SVM classifier shows the power in simply using the right threshold values when dealing with noisy data. Around a 6% increase in performance is achieved when using a threshold value of $1e-6$ as opposed to $1e-2$. It can also be seen that it is not simply a matter of making the threshold smaller or bigger, given that values too large ignore part of the desired signal, while values too small take into consideration too much of the noise.

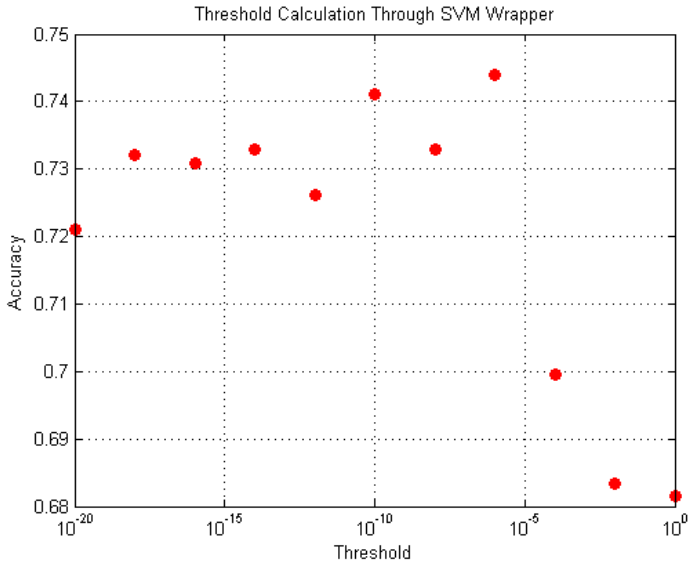


*Figure 22: SVM Wrapper Threshold Calculation*

The above study was further supplemented by using the previously defined Signal to Noise difference. Using this approach to extend the SVM wrapper results, it becomes easier to see how the optimal threshold value (that which maximizes signal content while minimizing noise), lies around the $1e-6$ mark. Furthermore, because this study was much less computationally expensive, a finer search for the threshold was possible, as is shown in Figure 23, arriving at the values specified below for each feature. It is these values which were used in the final classifier.

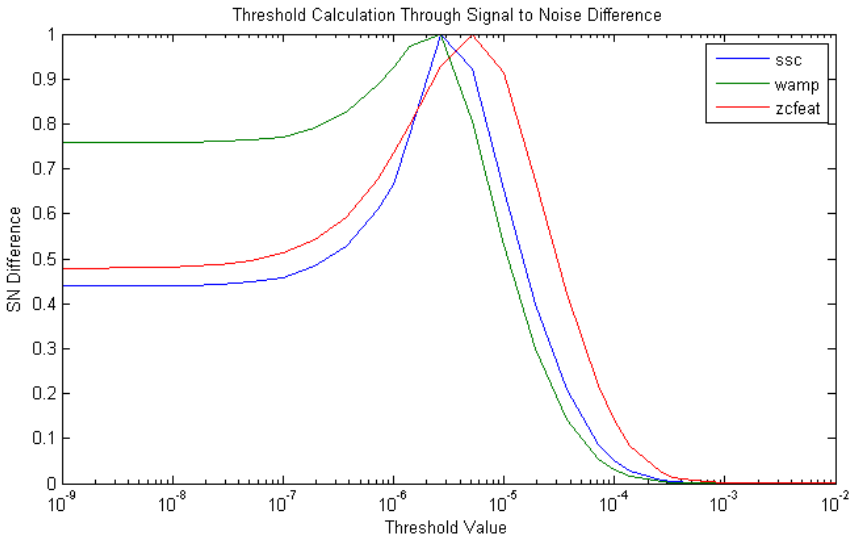


*Figure 23: Signal to Noise Difference Threshold Calculation*

$$\boldsymbol{ssc} = 2.68e-06 \qquad \boldsymbol{wamp} = 2.68e-06 \qquad \boldsymbol{zc} = 5.18e-06$$

### *5.2.2 Number of frames*

Another part of data representation which must be tested, lies in the number of frames an active segment must be split into. Splitting a gesture iteration into multiple segments is necessary for two reasons. First, most of the features being used deal with overall signal amplitudes. Even though this is exactly what we want, it also means that extracting features on whole signals can be misleading, as mirrored signals will have the exact same feature representation. Second, when it comes to gesture recognition, much like in speech recognition, much of the information that is sought comes from the temporal variations present in the signal. Because of these two reasons, it is detrimental to use a whole signal for feature extraction, instead the signal is broken up into a specified number of frames. In the case of HMMs, the signal is often split into frames of a certain time duration, however this leads to inconsistent feature vector lengths. On the other hand, in the case of SVMs which require equal size feature vectors, signals are split up into a set number of frames.

Once again using an SVM wrapper for average classification, a test was performed to study the effect of the number of frames in the overall system's performance. Figure 24 below show how once again, a simple change can have a consequential effect on performance. Simply varying the number of frames resulted in a

performance decrease of about 7%. These results will be used in the final model selection for both SVM and HMM classifiers.

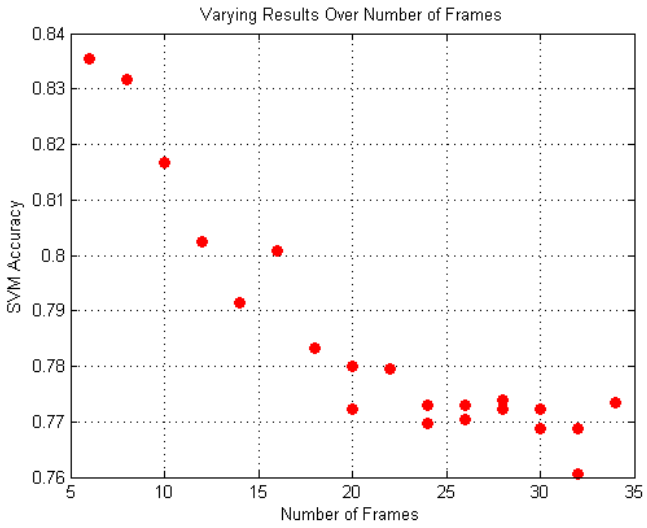


*Figure 24: SVM Wrapper Number of Frames Calculation*

### *5.2.3 Filter method feature selection*

After an appropriate threshold and number of frames have been selected, it is possible to turn more attention towards feature selection. As mentioned previously, feature selection is done for two reasons. First, features with little discriminative power can hurt the classifier as a feature can be consistent among all classes. If too many such features are used, the separability of each gesture class is put in jeopardy and performance declines. Secondly, at design and training time, too many features in the feature space can cause substantial computation issues which manifest themselves in long processing times.

The first approach tested for feature selection consists of a computationally light filter method. This method was used with two filters based on the Fisher Score and the T-test hypothesis. By using these two methods in conjunction, a reasonable feature ranking was achieved. Although this method is attractive for its ease of use and short computation times, it is not often used in the literature as the feature selection method of choice. This is due to its subpar performance when compared to wrapper based methods. Because of this, although the results shown in Figure 25 were taken into consideration as a first pass, they were put aside in the final classifiers, and instead the wrapper based selections were used.

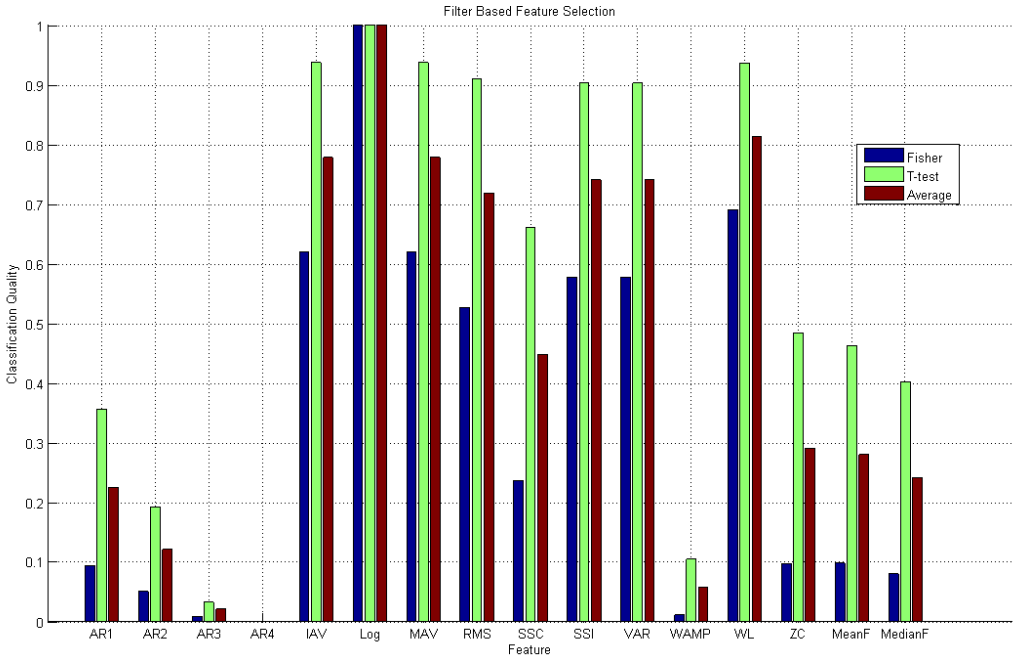


*Figure 25: Filter Based Feature Ranking*

**Feature Ranking:**

1. Log Detector
2. Waveform Length
3. Integrated Absolute Value
4. Mean Absolute Value
5. Single Square Integral
6. Variance
7. Root Mean Squared
8. Slope Sign Change
9. Zero Crossing
10. Mean Frequency
11. Median Frequency
12. WAMP
13. AR

### *5.2.4 Hidden Markov Model Wrapper*

Instead of using the filter feature selection results above, two wrapper based methods were tested using a HMM wrapper. Although these method resulted in much longer computation times, the reason why the wrapper method was used in place of the simpler filter method, is due to simple optimization. By using a HMM wrapper, it is guaranteed that the final feature representation for the data will be optimized for the HMM method.

The table below summarizes the results of the HMM wrapper feature selection. One detail to note is that during multiple runs of the same method, different feature

subjects were selected. This can be explained by the randomness in the cross validation training process. Furthermore, even though the feature subsets vary, it is important to note that average cross validation accuracy remains very consistent from run to run. The optimum feature subset was chosen as that resulting from the SFFS method. This result was a combination of best average accuracy and smallest subset. This result also goes to prove that the more computationally demanding SFFS method, gives the best results.

*Table 1: HMM Wrapper Feature Subset Scores*

| ACVR | Feature Subset | Method |
|---|---|---|
| 0.99 | ‘9,10’ | SFFS |
| 0.98 | '9,5,8,3,10,1' | SFS |
| 0.97 | '9,8,7' | SFS |
| 0.98 | '9,4,5,8,7,2,1' | SFS |
| 0.98 | '9,8,3,5' | SFS |

The feature subset values match to the following features

1. AR
2. Integrated Absolute Value
3. Log Detector
4. Mean Absolute Value
5. Root Mean Squared
6. Slope Sign Change
7. Single Square Integral
8. Variance
9. WAMP
10. Waveform Length
11. Zero Crossing
12. Mean Frequency
13. Median Frequency

### *5.2.5 Support Vector Machine Wrapper*

Likewise, the two wrapper based approaches were also used with a SVM wrapper for feature selection on the SVM classifier. This test also shows that the SFFS method provides the simplest and most robust feature subset.

*Table 2: SVM Wrapper Feature Subset Scores*

| ACVR | Feature Subset | Method |
|---|---|---|

| | | |
|---|---|---|
| 0.83 | ’12,11,9,6,5,10’ | SFFS |
| 0.83 | '11,12,9,4,6,3,5,2,10,7,8,13’ | SFS |
| 0.83 | ‘9,12,11,6,7,4,8,3' | SFS |

## 5.3 Dynamic Time Warping Results

Unlike HMMs and SVMs, the DTW classifier does not require much fine tuning. Instead, only the data preparation method and the number of iteration examples are required. Two tests were conducted to arrive at the optimal values for these two parameters. From these the optimal test was consolidated and conducted. Finally, the optimized test results served for calculation of the ACVR, ARR, and APR (for the definitions of these values, refer back to section 5.1); as well as for comparison with the SVM and HMM classifiers.

### *5.3.1 Number of Examples and Data Preparation Test*

In order to calculate the optimal number of training examples for the DTW method, a series of tests were conducted with increasing number of examples. These tests showed that the method, although simple in theory, requires large computation times. In fact, tests with more than 15 training examples took such a long time to run that they had to be aborted due to time impracticalities. Hence, the number of training examples was set at 15, the largest value which was feasible for training multiple versions of the classifier. This number matches what other researchers have found for similar data types [17]. In practice, this number of class examples is also a lot more feasible than the other two classifiers are likely to need. For instance, if an amputee is to train a personal prosthetic, any more than 15-20 iterations might prove too tasking and decrease the user experience.

The choice of the optimal method of data representation was found by conducting two simultaneous experiment of DTW using both methods in question. Both experiments were conducted using the same 8 classes out of the 18 class gestures in order to minimize the computational complexity of the method. Both experiments were also conducted using the same 15 example iterations out of the possible 138 iterations available through the Ninapro dataset.

The results which are shown here compare the SAX and down sampling methods in two fronts. First and most important the ACVRs are compared. Secondly, the time taken for training and classification are also compared. This second comparison is done in order to reiterate that classification accuracies are not the only important parameter when choosing a classification method. Training time which is a large portion of the setup time for this method, and classification time, which will dictate how the system responds to online inputs, are also monumentally important to the end user experience and to how the system will operate.

Table 3 below shows the DTW results using the SAX method. The ACVR, training and test time are shown on a per-class basis. Training times shown here are the times required to pick a template out of the possible 15 iteration examples. The classifying times on the other hand are presented as the time to classify all 15 iterations. Thus with an average of 43 seconds as the classifying time, a single gesture takes roughly 2.8 seconds for classification. The next important set of results for the SAX method are the ACVR, APR, and ARR. Of the three classification statistics, the ACVR is the most meaningful in terms of choosing a method of choice. The result of the SAX data preparation method is a mere 34%.

*Table 3: SAX vs. Down Sampling DTW*

| Method | ACVR (%) | Average Training Time (sec) | Average Classifying time per Example (sec) |
|---|---|---|---|
| SAX | 34 | 43 | 43 |
| Down Sampling by 3 | 36 | 2829 | 1429 |
| Down Sampling by 5 | 35 | 802 | 495 |
| Down Sampling by 9 | 30 | 255 | 154 |
| Down Sampling by 13 | 23 | 121 | 64 |

The second method which was studied in conjunction with the DTW approach consists of down sampling and filtering the data before it goes into processing. The only variable to this method is the down sampling factor which was varied from 3 to 13. As the table above also shows, this method does not improve on the SAX method. Furthermore, even though there is a good bit of down sampling happening, training and classifying times are still too large for this method to be of any practical use.

### *5.3.2 Final Model*

After the comparison of the two data preparation methods above, and the choice of a number of class examples, a final test was conducted in order to calculate the final ACVR, APR, and ARR for the DTW classifier. This classifier was also tested using both the null class and the null threshold methods covered in the methods section. A comparison was made of which of the two approaches provide the best performance when classifying EMG data which includes low activity time.

The first statistic of importance when evaluating a classifier is its power to classify different classes. Using the k-fold approach for noise reduction during the training phase, the confusion matrix in Figure 26 was calculated. It, along with the precision, recall, and average cross validation ratio shown in Figure 27, demonstrate the inadequately low classification power of the DTW method to noisy EMG data.

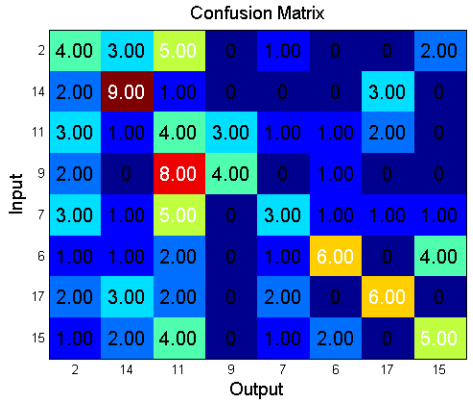


*Figure 26: DTW 8 Class Confusion Matrix*

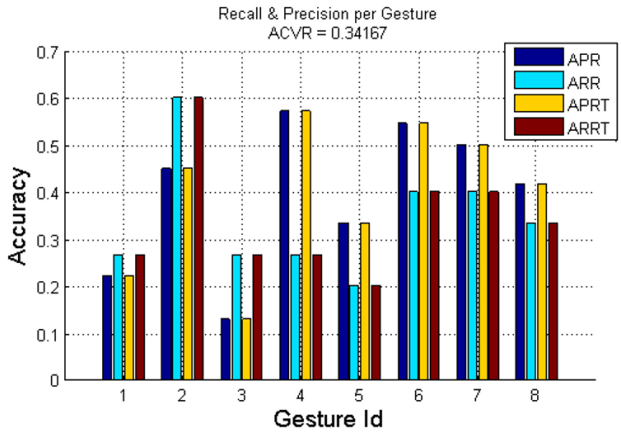


*Figure 27: DTW 8 Class Precision and Recall*

Figure 27 also shows that it is not only the overall classification score that is extremely low, but also the classifier's recall and precision to individual classes. These values will later be used to compare and contrast the DTW classifier against the SVM and HMM classifiers.

It is also worth recalling that the results above are those of 8 out of the 18 possible gesture classes available. The results show an even further decreased performance (with an ACVR of 18%) when the number of classes increases; this further decrease in performance can be seen in Figures 28 and 29 below.

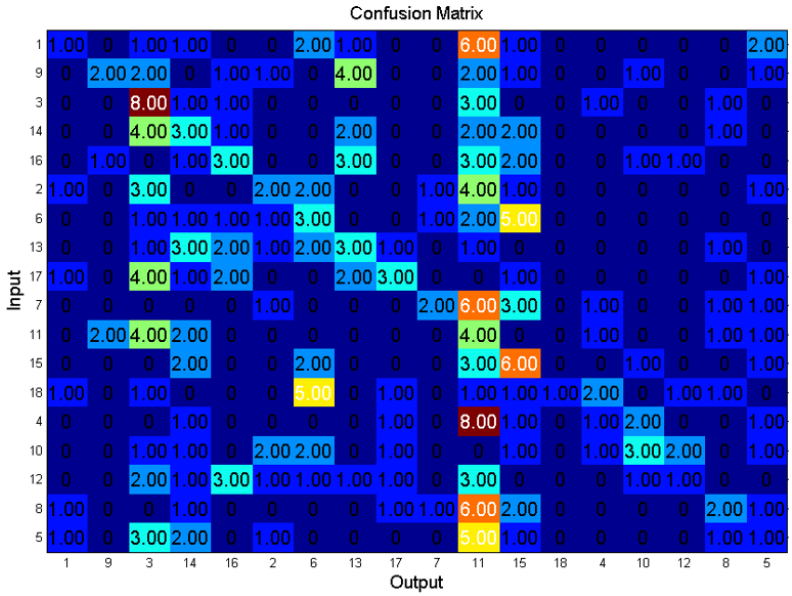


*Figure 28: DTW 18 Class Confusion Matrix*

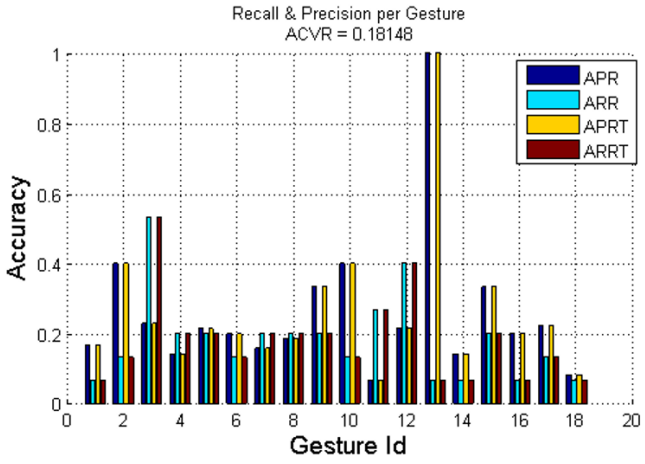


*Figure 29: DTW 18 Class Precision and Recall*

One last comparison and deduction that must be made from these results is that of the null class vs the null threshold. It turns out that due to the wide variance of the intra class distances between iterations, both the average and the standard deviations values which go into making up the threshold value for each class are larger than the distance values at classification time. Due to this and the fact that inter class distances are not large enough, the threshold value does not in fact make any difference to classification. That is to say, that once a classification has been made, the null threshold fails to remove even one false classification from the set.

At the same time, the null class method did not fare any better in improving performance. Instead, null class examples (gesture 18 in the above confusion matrix) get distributed amongst other non-null classes. In practice, this would equate to false gestures being performed during rest times. Through this quick analysis it is possible to see how neither of the approaches aids the DTW classifier. Ultimately, if a choice between the two is to be made, the null threshold would win out over the null gesture given that it does not add to the time complexity of training in the same way that an extra class would.

### *5.3.3 Issues with Dynamic Time Warping Method*

The DTW classifier fails to be a feasible solution to the Ninapro dataset due to two main issues: long training times and lack of class separability. Training times are long due to the need for multiple grid searches over the 2 kHz sampled signal. When a gesture can take anywhere from 2 to 5 seconds at a 2 kHz pace, this equates to a grid search on a 4,000 x 4,000 grid at a minimum and a 10,000 x 10,000 grid at a maximum. This issue is only emphasized by the multidimensional nature of the EMG signals. The issue of separability is a result of the noise in EMG signals making them look like each other. This problem can be seen in the Figures 30 and 31, where the first of the two plots show DTW distances for each iteration of a single gesture, while the second shows the DTW distance from each misclassification to the correct template for all iterations over all gestures. In the Figure 30, every iteration should have been classified as belonging to template 2, instead it shows how DTW distances across all templates are very similar. Meanwhile Figure 31 shows the distance from each iteration classification to its correct classification; for instance, the value of 0.79 for gesture 11 iteration 44 refers to a gesture

iteration for class 11 that was misclassified to a template with a DTW distance 0.79 smaller than its own template. Together these two figures show that there is no inherent separability between gestures in the down sampled space (be it through SAX or decimation). Furthermore, this issue is also magnified by a detail of DTW; mainly that the version of DTW used in this work requires that the signals match up at the start and end of the grid search. This means that unless movement iterations start and end at similar moments, the signal distance is due to be thrown off. All of this results in bad classification performance.

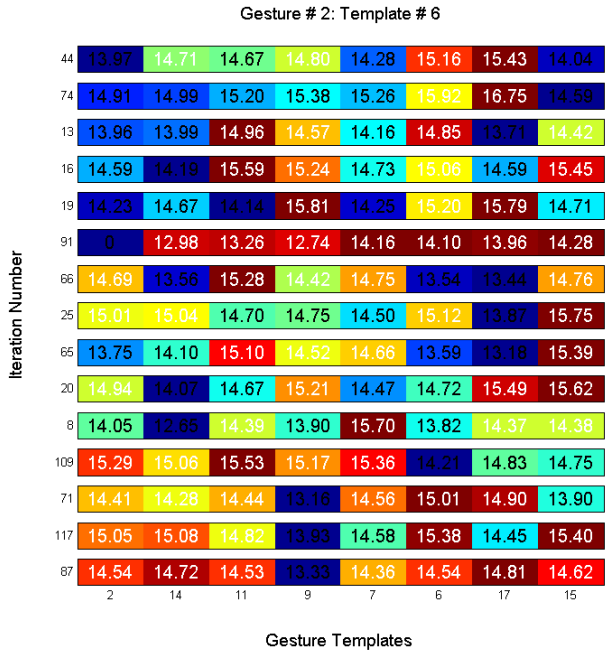


*Figure 30: Gesture 2 Iteration Distances from Templates*

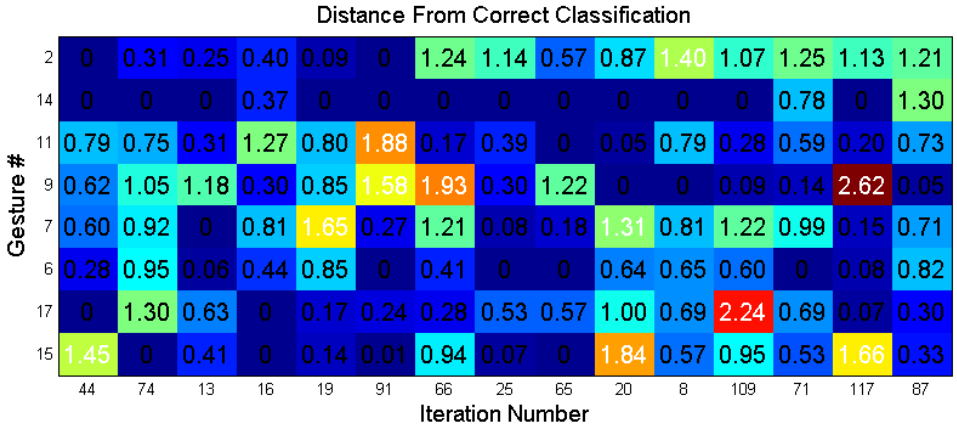


*Figure 31: Example Misclassification Distances*

A solution to the first issue might be to down sample to data, however, this was studied in the previous section and found not to produce reliable performance. The reason for this might be that down sampling was done through decimation. This might also be a reason why the SAX method performed better than down sampling, since it 'down samples' in a smart way. As for the second problem, a version of DTW might be presented in which the requirement for a full data grid is relaxed. This might create more cohesion between class members while distinguishing different classes.

## 5.4 Hidden Markov Model Results

In order to set the optimal parameters for the HMM gesture classifier, the following experiments were conducted. Each test is designed to optimize one HMM parameter. The first, finds the optimal number of states and emission observations for the model. The second tests the assumption that left to right models are optimal when compared to ergodic models. The third and fourth test for the classifier's power to distinguish between a range of classes, and the minimum amount of information required for training. Finally, all these tests are combined and tested in unison. The SAX discretization approach is also tested and compared to the feature extraction approach.

### *5.4.1 Model Setup*

The first test conducted for the HMM classifier aims to find the optimal number of states and observations for the model. In the case of gestures, a state in a HMM could also be considered the step during a movement sequence, while an observation is the EMG data that is collected by the sensors and recorded.

This test while only the first one conducted specifically for HMM, is also one of the most important. The importance of these two parameters can be seen in Figure 32, which shows the average cross validation results for the grid search conducted.

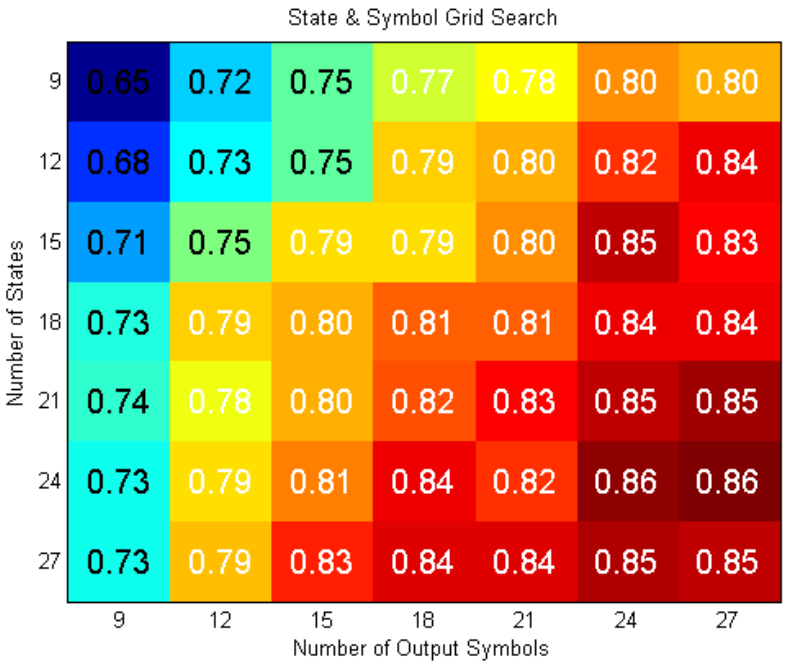


*Figure 32: HMM States and Symbols Test*

As can be seen in the matrix above, validation results vary around 20 percentage points based solely on the number of states and output symbols used. Looking at the number of states in the model, it is apparent that the optimal number of states for the data being studied is around 24. A much smaller number of states fails to properly separate the steps of a gesture and underfits the data, thereby confusing gestures with each other. While on the other hand, too many states overfit the data and adds computational complexity while not improving classification. The same analysis holds true for the number of output symbols in the model. The optimal number of emission symbols for the current system is also around 24. The final and optimized HMM classifier will be tested with both 24 states and output symbols.

### *5.4.2 Left to Right vs. Ergodic Models*

As was covered in the HMM background section, there are different types of state interactions allowed in HMMs. These types range from the very general ergodic model in which all states are allowed to transition amongst themselves, to the more restrictive left-to-right model which is often preferred in speech and gesture recognition, but only allows monotonically increasing state transitions. Though this work began with the assumption that a left-to-right model would be optimal for gesture recognition, a test was nonetheless

conduced for the flexibility such a model would provide. In order to perform such test, the left-to-right structure was modified in such a way that state transitions would be allowed to skip over an integer number of states.

The results of these series of tests, which can be seen in Figure 33, show that although a small amount of generalization is favorable, increasing the classifier's performance by 4% points overall from no allowed skips to 4 skips, there's really not much to gain from allowing too many skipped states. These results seem to corroborate what other researchers have already indicated, that a left-to-right model is optimal for gesture recognition.

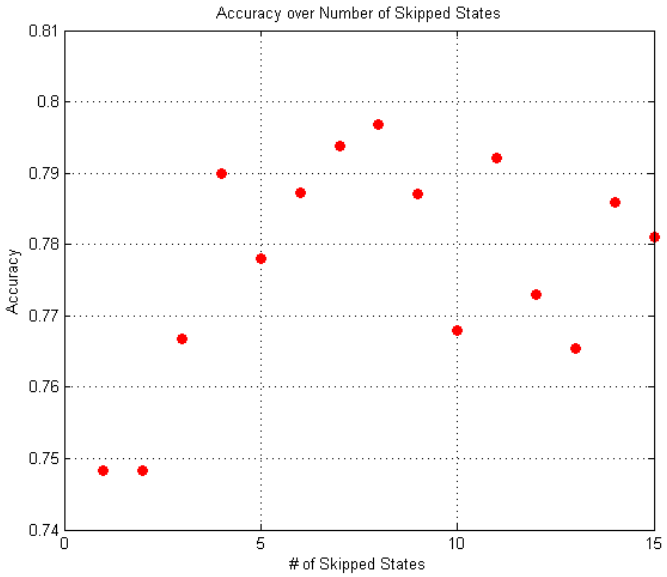


*Figure 33: HMM Number of Skipped States Test*

### *5.4.3 Effect of Increasing Vocabulary*

This test was designed and conducted to gauge the power of the HMM classifier under different number of classes. As discussed previously, this is important when looking into the end user goal, be it sign language recognition, military hand signs, or others.

As one would expect of this kind of classifier, performance decreases with increasing complexity. Figure 34 shows that HMM performance declines around 10% points when classifying 18 gesture classes as compared to only classifying 6 classes. Although this result is what was expected, it is always a good sanity check to make sure that a classifier is doing what's expected. Furthermore, because this test was performed

with a number of variations, the results also go to show something that has already been proven, that a 24 state model outperforms a 15 state model in average cross validation.

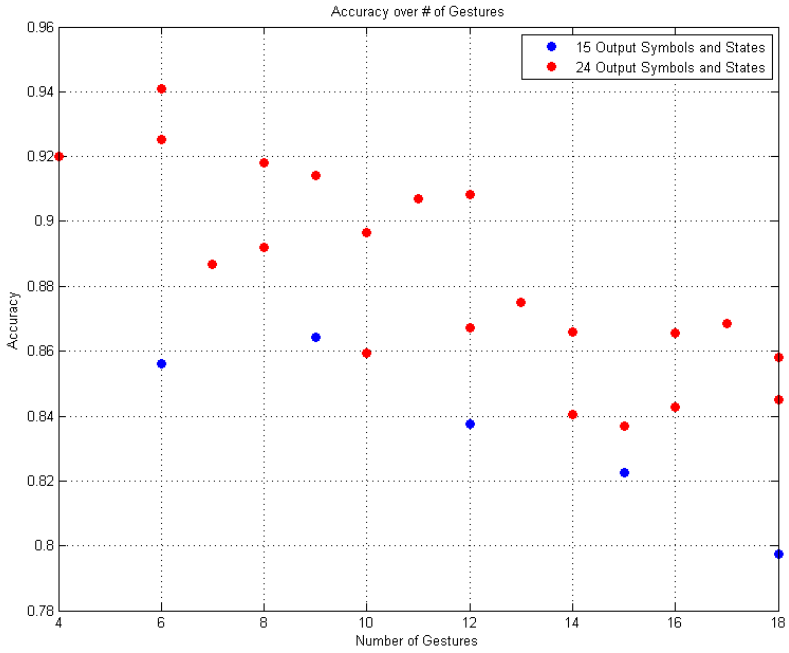


*Figure 34: HMM Accuracy Over Number of Classes*

### *5.4.4 Minimum Required Training Data*

The following test was performed for estimating a minimum number of training observation required for proper HMM operation. Previous works have hinted at around 70 training observations being necessary for training a Hidden Markov model. This number is consistent with the outcomes of this test, which are depicted below.

As can be seen, a HMM's performance rapidly increases at small amounts of training data; increasing the training set from 10 to 20 observations increases performance by roughly 15% points, and adding another 20 training instances, adds another 15% points. However, this rate of increased performance is not consistent when adding more data samples. Instead, the learning curve reaches a semi plateau at around 80 training samples, where much more data improves the classifier's performance in a disproportionate rate to the of growth in computational complexity.

Figure 35 shows results for a number of runs of the HMM classifier under different conditions. These conditions vary not only in the number of training samples, but also the representation of the data, the feature subset, the number of states and

symbols, and even the number of allowed skipped states. Though labeling these different runs is not an important outcome of this test, the graph nonetheless does a good job at demonstrating that even under very different conditions, HMM classifiers still follow the same general learning curve and require around the same amount of training data.

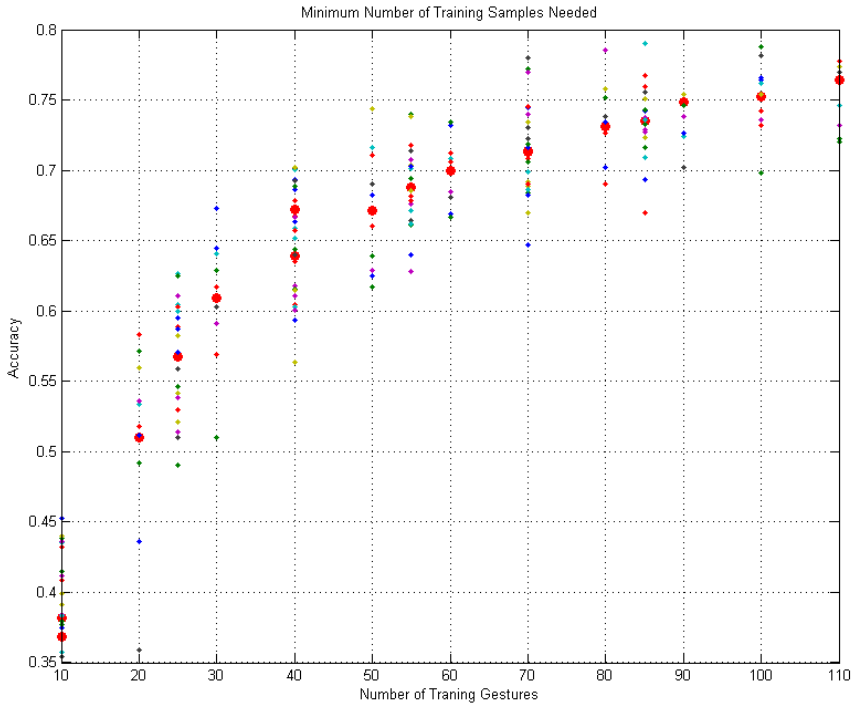


*Figure 35: HMM Minimum Amount of Training Data*

### *5.4.5 Final Feature Model*

After having gone through the previous tests for each important parameter of a HMM classifier, it is finally possible to conduct a final test with all the optimized selections. From the previous results the parameters of choice are:

- SFFS feature subset
- Four allowed skipped states
- Closest cluster discretization for testing
- Uniform kmeans start in discretization for training
- 24 output symbols and states
- Tenfold cross validation with at least 80 training observations

Apart from these settings it is also important to settle on a model for the null gesture. The decision of whether to use the threshold mandated nullifying process or to implement a null class based on inactive or undesired segments depends heavily on the data and the variance of various repetitions of a single gesture. Previous works into EMG controlled devices have found that the threshold method worked well for discarding null EMG segments [17]. However, other works point at the fact that this decision is truly case per case dependent and should be studied based on the data available. Hence, the following tests were designed to compare and contrast the use of the threshold vs the null gesture class method. For each experiment the APR and ARR were calculated on a per class basis as well as the ACVR for the overall process. The results, which are shown below in Figure 36, demonstrate that for the data being tested here, the threshold method (APRT, ARRT, ACVRT) results in decreased performance. On the other hand, the null gesture class method (APR, ARR, ACVR) keep the ACVR above the 90% mark as in previous tests. From these results it can be concluded that for the Ninapro dataset, which is inherently noisy, the null gesture model method is the optimal solution.

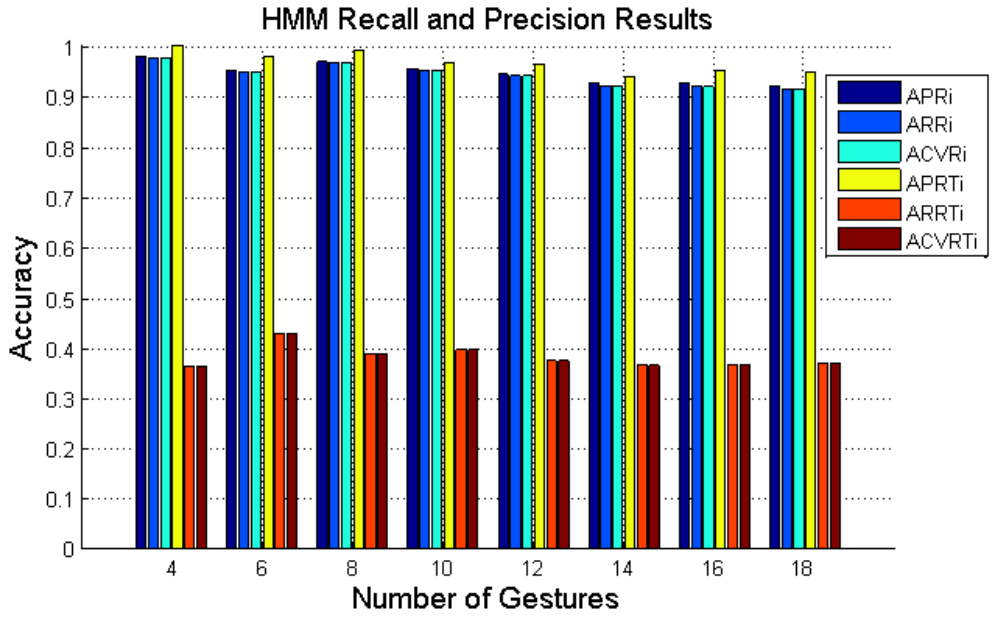


*Figure 36: HMM Recall and Precision Test*

Using these settings, a final test was conducted over a varying number of classes. The results below show how the optimized model (Figure 37) improves on the previous

iteration of this test (Figure 38). From these two table it is once again possible to see how the ACVR lies reliably above the 90% mark, and close to perfect classification at a small number of gestures.

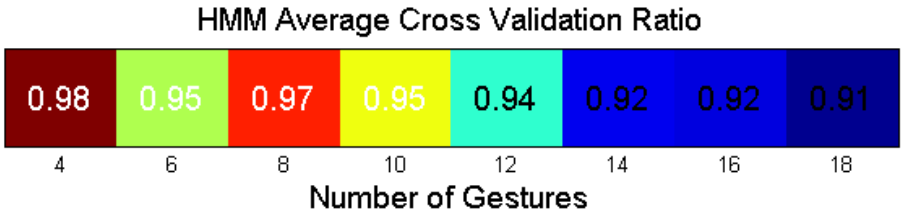


*Figure 37: HMM Optimized Results*

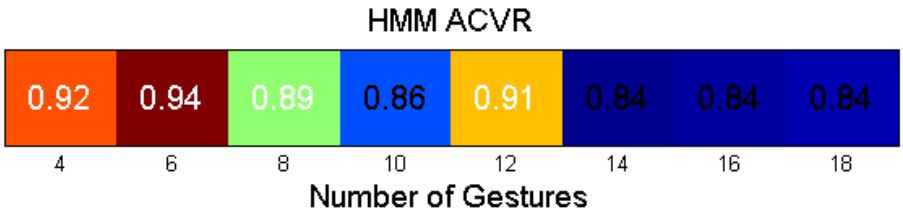


*Figure 38: HMM Sub-Optimal Test*

Additionally, the APR and ARR were also calculated on a per class basis. From the results shown in Figure 39 (whose ids match the gestures detailed in Figure 40), a designer could give feedback to the user and recommend that certain kinds of motions be avoided.

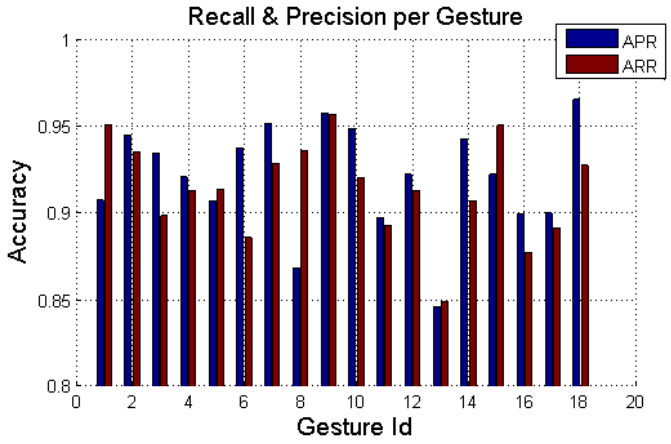


*Figure 39: HMM Gesture Separability*

| | # | Description |
|---|---|---|
| Hand and wrist movements | 1 | Thumb up |
| | 2 | Extension of index and middle finger while flexing others (cf. "V-sign") |
| | 3 | Flexion of ring and little finger while extending others |
| | 4 | Thumb opposing base of little finger |
| | 5 | Abduction of the fingers |
| | 6 | Fingers flexed together in fist |
| | 7 | Pointing index |
| | 8 | Adduction of extended fingers |
| | 9-10 | Wrist supination and pronation (rotation axis through the middle finger) |
| | 11-12 | Wrist supination and pronation (rotation axis through the little finger) |
| | 13-14 | Wrist flexion and extension |
| | 15-16 | Wrist radial and ulnar deviation |
| | 17 | Wrist extension with closed hand |

Figure 40: Movement ID and Descriptions, A. Gijsberts, M. Atzori, C. Castellini, H. Muller, and B. Caputo, "The Movement Error Rate for Evaluation of Machine Learning Methods for sEMG-based Hand Movement Classification," *Neural Syst. Rehabil. Eng. IEEE Trans.*, vol. PP, no. 99, p. 1, 2014.
Used under fair use, 2014.

### *5.4.6 Final SAX Model*

Though most of this work has concentrated on vector discretization through the extraction and clustering of feature vectors, a series of tests were also conducted on the alternative form of data discretization called SAX. As covered in the background section, SAX is a method through which a signal can be discretized, and through this discretization, also simplified and filtered. By setting a number of frames, and a vocabulary size, it is possible to get rid of a lot of the noise in the signal.

The confusion graph in Figure 41 shows the initial results of the SAX implementation running through a HMM classifier. As can be seen in the graph, SAX discretization works very well for EMG gesture recognition, even better than the alternative discretization through feature extraction. One of the reasons for this improvement probably lies in the fact that the selected features might not adequately quantify all the information in the EMG data. Although, care was taken to find the most prominent features in the literature and to select the best of those through feature selection, it is unfeasible to test all the possible features and combination of them against the HMM wrapper. Thus, a truly optimized model is difficult to reach. On the other hand, SAX discretization does not depend on specific features, but rather uses the waveform itself to create a model. This fact plus the inherent noise filtering that takes place through proper vocabulary sizing means that SAX discretization might actually capture more of the intricate details of the EMG data.

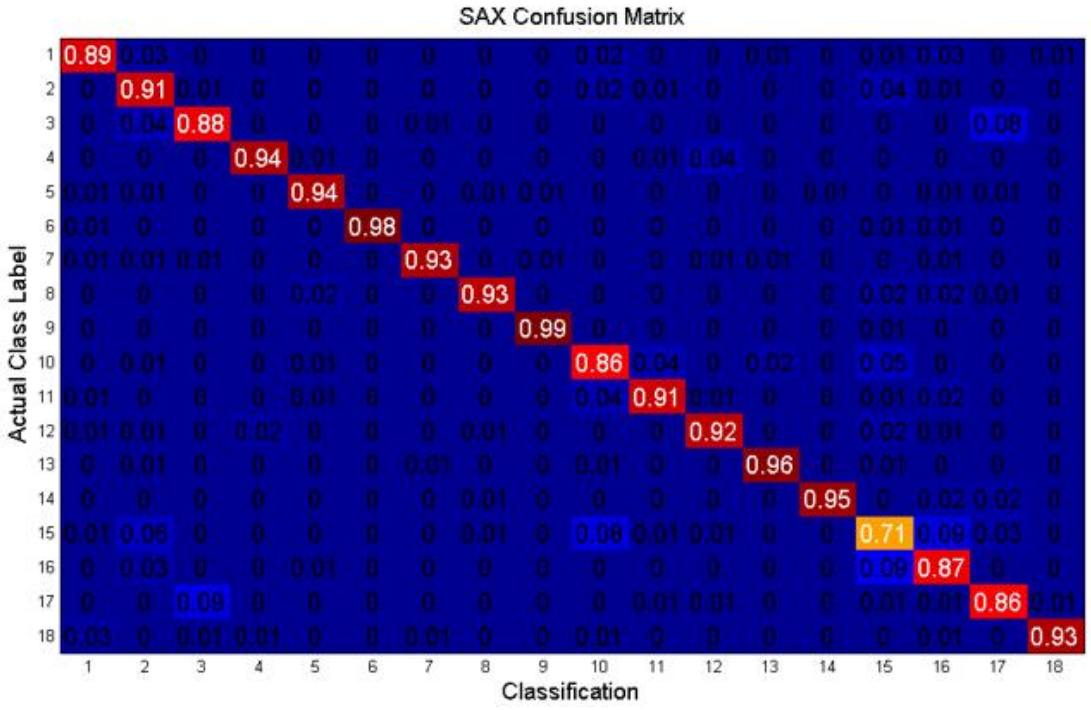


*Figure 41: SAX Discretization Confusion Matrix*

These results can be further expanded into an average recall and precision ratio per class. This study is shown below in Figure 42, and demonstrates the power of the SAX HMM classifier to distinguish each class. Through this analysis, it becomes possible to provide feedback to the user as to which gestures lend themselves to higher quality results.

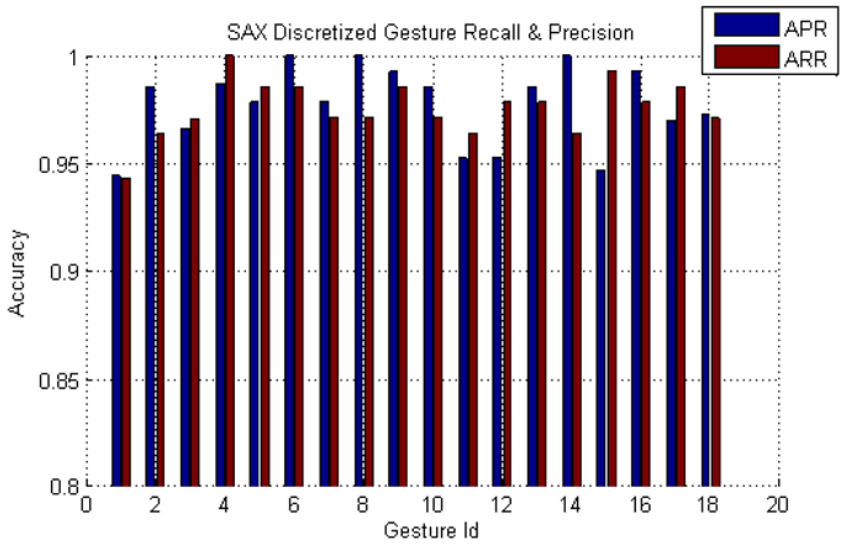


*Figure 42: SAX Discretized Recall and Precision*

As a way to double check the accuracy of the previous method and of all HMM tests in this section, two more tests were conducted using the SAX discretized data. The first is a test which only uses the information from one user for training and testing. This test simulates a scenario where a single end user would be setting up and using a gesture controlled device, be it some sort of generic human machine interface, a prosthetic, or other scenario. The second test is a very general training technique in which training and testing data has also been broken up by subject. In other words, data from each subject has either been used entirely for training or testing. This is in contrast to the method that has been followed up until now, where each subject's gesture repetitions could be split randomly into training and testing. The rationale behind these two tests are to check for over and under fitting of the model. Test one is based on the idea of over fitting a model to a specific subject, while on the other hand, test two tries to negate any subject specific over fitting which might be taking place in the random approach.

Figure 43 below shows the result of test number one, where only a single user was used for training and testing. The graph shows the average cross validation ratio for each of the 23 subjects whose data was chosen. As can be seen from the graph, the single user data is not very accurate. This is probably due to the fact that there is a very small amount of training samples. Per every user, and per every class, there are a maximum of five training examples in Hold one out cross validation. These five training samples are not enough to properly train the HMM, as was seen in previous sections. In cases such as this one, where training samples are small per user, a mixed training method, where training samples from multiple users are mixed for training is optimal.

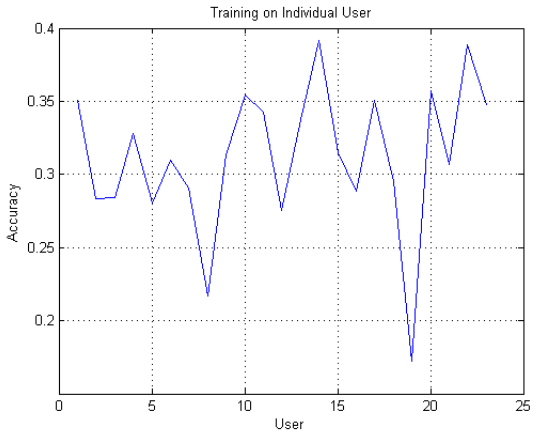


*Figure 43: SAX Individual User Results (Overfitting)*

In the case of the second test, it is assumed that multiple users have provided data either for testing or training. As can be seen in Figure 44 even when completely avoiding over fitting to a specific subject, given enough data SAX HMM classifiers are very powerful at distinguishing amongst different gestures. Furthermore, because the SAX learning curve below seems to follow the learning curve in the previous section, and the result for a single training user (6 training observations) matches the result for test one previously conducted, it is possible to say that over fitting is not in fact a large source of error in these series of HMM tests.

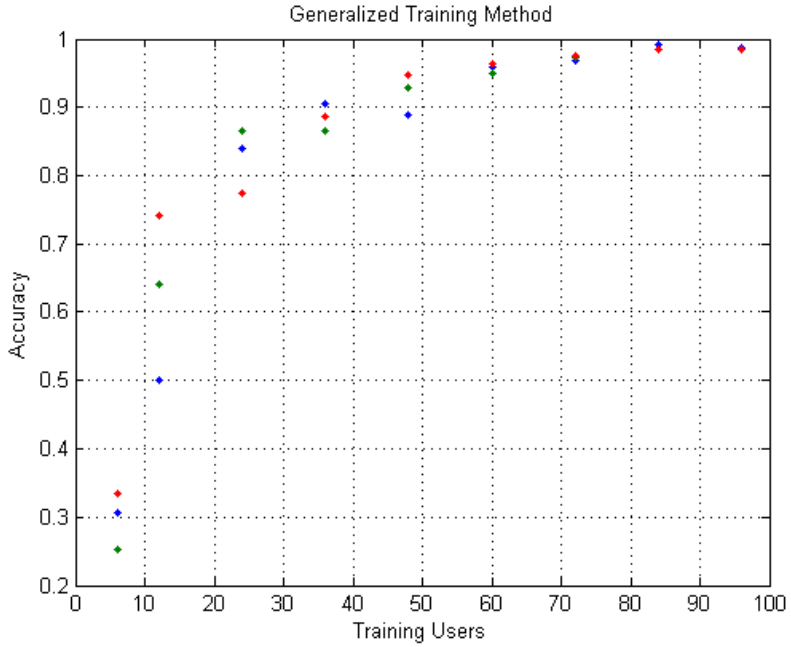


*Figure 44: SAX General Test (Underfitting)*

## 5.5 SVM Results

Much like the HMM classifier, SVMs also require the fine tuning of certain parameters for optimal performance. In this case, these parameters consist of the choice between kernel function, for the so called ‘kernel trick’; the pinpointing of the kernel function’s parameters; the identification of the classifier’s power to a number of classes; and the amount of training data required for proper performance. In order to test each of these parameters, the following series of experiments were conducted, each of which

optimizes one of the desired parameters. These findings are then combined in the final SVM test, which is also used for calculating ACVR, APR, and ARR.

### *5.5.1 Kernel Test*

The first task to be completed for the SVM classifier, is the decision on what type of kernel function to use. The EMG literature shows examples of the use of both the linear and RBF kernels in gesture recognition. Although the RBF kernel is much more prevalent among researchers due to its robustness when compared to its linear counterpart, the simpler linear kernel is also often used as a comparison point for classification. It is with this goal in mind, that the linear kernel is used here.

The first step of the kernel experiment consisted of running a benchmark test using the linear kernel. As mentioned in the background section of SVM classification (refer to chapter 3), linear kernel in SVM classification is often used as a comparison tool for other kernels, as it is often equivalent to non-kernel versions of an algorithm. The graph below shows a grid search approach conducted with a linear kernel. As a reminder, the linear kernel is calculated through the equation:

$$H(x, x') = x^T * x'^T + c$$

As such, parameter c was iterated through powers of two. As Figure 45 shows, the linear kernel is not much affected by the c parameter, and gives a constant classification result of 79%.

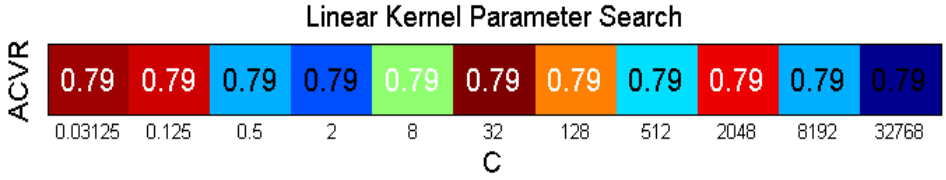


*Figure 45: Linear Kernel Average Cross Validation Ratio*

With this as a benchmark of the simplest case, the popular RBF kernel given by:

$$H(x, x') = \exp(-\gamma||x - x'||^2)$$

was also tested. In this case, the $\gamma$ parameter was also iterated through a grid search ranging from $[2^{-15} \ldots 2^3]$ and shown in Figure 46. The results of this test show that the RBF kernel is both much more dependent on its parameters and powerful than the linear kernel. At the most optimal case found, the RBF kernel achieves a performance of 88%

correct classification. As such, it is this kernel that was used on the final SVM classification test.

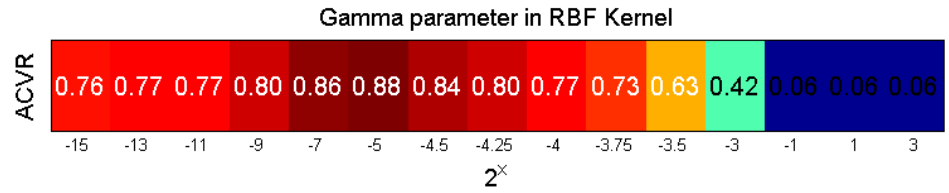


*Figure 46: RBF Kernel Parameter Search*

### *5.5.2 Effect of Increasing Vocabulary*

Since the result of the previous test show that the RBF kernel outperforms the linear kernel, this follow up test was conducted using said kernel. It was also conducted using 10 fold cross validation as a means to minimize random noise effects in the training procedure, and a large enough number of samples for proper training.

The results for this test, shown in Figure 47, demonstrate a similar pattern to the HMM classifier. Performance decreases with an increasing number of classes, with classification accuracy declining roughly 15% from 4 to 18 classes. Furthermore, even through the random nature of training and testing, it is still possible to see a clear linear decline in performance as the number of classes increases.

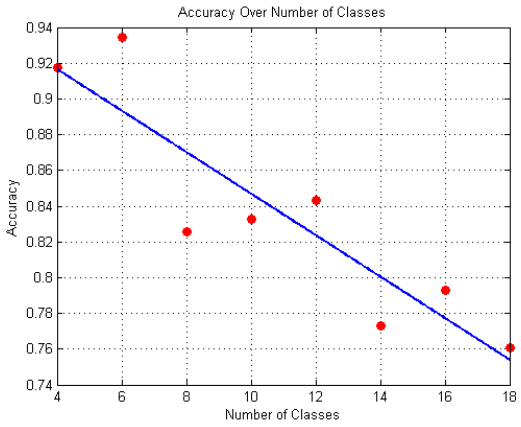


*Figure 47: SVM Performance vs. Number of Classes*

From these results, it becomes possible to weight the necessity for a certain amount of classification power against the number of classes needed for a certain end goal. For instance, if these result represented the final SVM classifier, then this sort of approach would not be recommended for a use such as ASL recognition, in which a

greater number of classes is needed. On the other hand, if the goal required a smaller number of classes, the current SVM classifier might be enough.

### *5.5.3 Minimum Required Training Data*

Figure 48 shows that there is a minimum number of training data needed for classification. In the case of both the linear and RBF kernels, this number hovers around the 90 sample mark, at which point there only minimal improvement in comparison to the computational complexity which results from increased amount of training data. As with the HMM method, there is also rapid growth with small amounts of data. This hints at the fact that in the case where only small amounts of data is available, efforts should be made to collect more data.

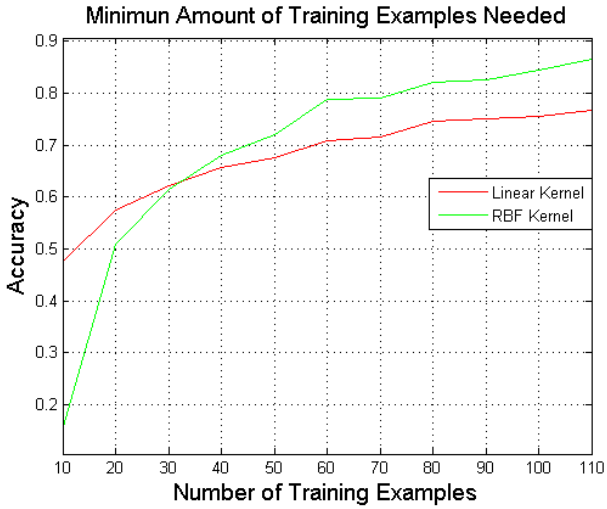


*Figure 48: SVM Learning Curve*

### *5.5.4 Final SVM Model*

After the series of tests to optimize different parameters of SVM training, a final model was constructed by joining the optimized results of each test. First, the SFFS version of the data was chosen as the most powerful and simple representation of the EMG data (please refer back to section 4.1 for the detailed feature selection test). Also, as a choice of data representation, 7 frames were chosen as the optimal number with which to split the data. This number of frames, though in contrast to larger values proposed in the literature, is the value that optimized results during the tests conducted in this work. Furthermore, from the experiments in this section, the RBF kernel with a gamma parameter of -5 was chosen over the linear kernel as a more robust version of the

algorithm, with a classification accuracy of 88% in the non-optimized test. And finally, 10 fold cross validation was used as a means of both reducing the effects of random noise in the training method as well as utilizing enough samples for proper training.

The results in Figure 49 show that by combining optimization results from each test, the SVM classifier becomes very powerful to EMG classification. By comparing these results to those in section 5.5.2, it is possible to see how the results improve drastically even at a large number of classes.

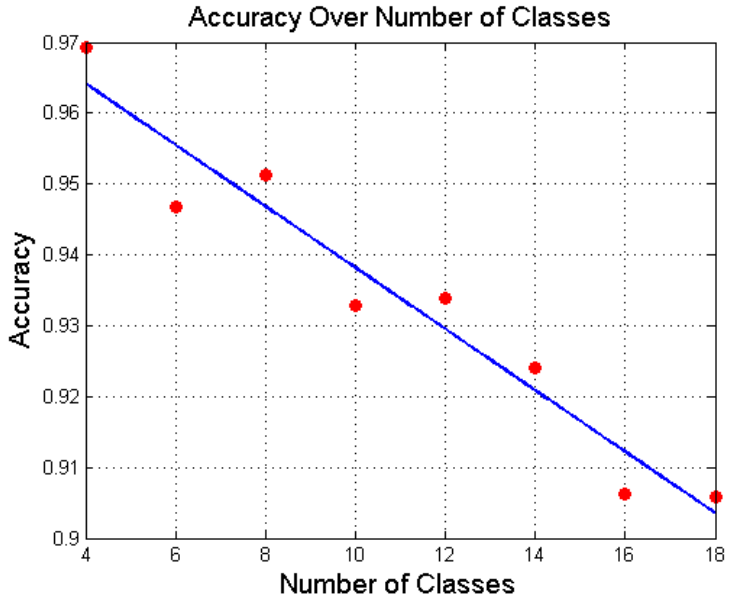


*Figure 49: SVM Optimized Average Cross Validation Ratio Results*

The average precision and recall ratios were also calculated per each of the 18 classes studied, including the null gesture. From Figure 50 one can see some movements lend themselves much more to be distinguishable through the SVM classifier. In real operation, it is these movements which would be optimal when establishing the class dictionary.

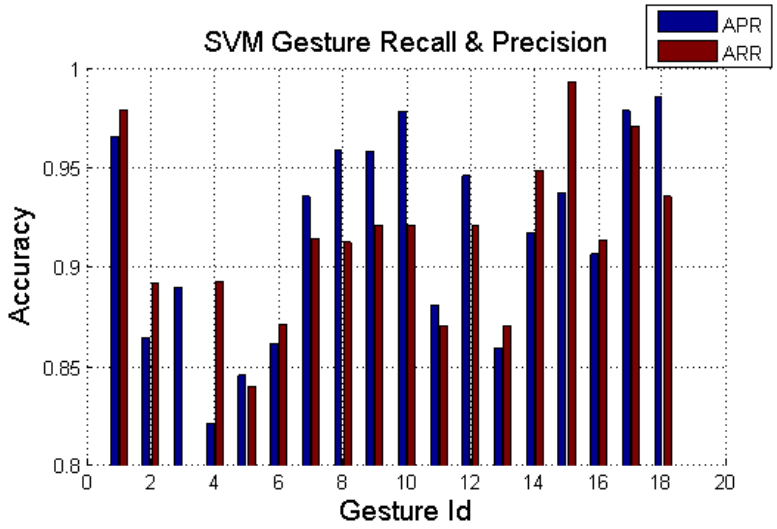


*Figure 50: SVM Optimized Recall and Precision*

## 5.6 Summary

Chapter 5 has presented the experimental results for each of the experiments set forth in the previous chapter. These results begin with data representation, and go through each of the three learning methods in question. Through these results, optimized models were also formulated based on the collective results of the experiments. These results are compared where appropriate, and will be further discussed in the following chapter. Furthermore, this chapter has also outlined a way to score, compare, and contrast classification accuracy, as well as the detailing how to read the plots in this and the following chapters.

# 6 Conclusions

## 6.1 Chapter Summary

After reviewing all test results, it is possible to go back and interpret them in the context of the initial problem formulation. This thesis deals with the comparison of three distinct classifiers for human gesture recognition and their optimization for the Ninapro dataset. This dataset is a new benchmarking tool which continues to gain traction amongst gesture classification researcher for comparison of different tactics. As such this chapter will first cover the results offered by other researchers with the same dataset, then it will compare the three classifiers chosen for optimal operation, it will cover the final achievement towards gesture classification, and finally will cover future work which might result from this analysis.

## 6.2 Previous Ninapro Results

The Ninapro dataset is quickly becoming popular as a tool for comparison. Since its latest version was released in 2014 with the work entitled "Characterization of a Benchmark Database for Myoelectric Movement Classification", multiple researchers have applied a number of classification tools to the set and reported their results [49]. Although not a comprehensive list, the results taken from the Ninapro website are detailed below. These results show a sample of the different approaches taken by researchers, mainly the use of k-nearest neighbors and linear discriminant analysis. The table also shows that thus far, of the classification results available through the Ninapro website, the maximum efficiency achieved has been 83.5%. These results will be used for comparison of the classifiers used in this work.

*Table 4: Ninapro Classification Results*

| Classification Mode | Procedure | Movements | Classification Results (%) |
|---|---|---|---|
| Intra Subject | Custom Acquisition Procedure | All, rest included | 83.5 |
| Intra Subject | k-nn | All, rest included | 55 |
| Intra Subject | multi k-nn | All, without rest | 50 |
| Intra Subject | multi k-nn | All, without rest | 52 |
| Intra Subject | LDA | All, without rest | 40 |

For the three classifiers tested here, there are two important aspects which must be explored. The first consists of the time required for training and classification using each

method. This parameter is important for two reasons; first, during development time when multiple methods and versions must be tested, long training times would be inefficient and reduce the number of possible test iterations, thereby reducing the possible scenario searchers and possibly occluding the optimal result. Secondly, after a system has been deployed for consumer use, classification times will mandate the time the system requires to make a classification, which in turn will mandate the responsiveness of the system and its ease of use for the subject. The second parameter which will be explored is the system's classification accuracy. These results are obviously important given that low accuracies demonstrate the inability of the algorithm to recognize a gesture.

## 6.3 Thesis Results

First, let's take a look at training and classification times for the three classifiers. Figures 51-53 below demonstrate the performance of the SVM, HMM, and DTW methods respectively. Due to the time complexity of each method, the results for both the SVM and HMM classifier are shown as an average over a number of different gestures from 4 to 18 gesture classes; however, for the DTW method which required the most training time, results are shown are only for the 8 class set. In order to compare the three outcomes, it is necessary to compare the SVM and HMM 8 class gesture result, with the DTW result. These times immediately show how although both the SVM and HMM classifiers might be possible contenders for real time classification, the DTW method requires of too much time for training and classification. As covered in the DTW section, in an ideal situation some of the training burden could be removed through down sampling, however the Ninapro dataset does not show much improvement even after down sampling by a factor of 13. These result alone are enough to remove the DTW method from contingency as a possible classifier for the Ninapro dataset.

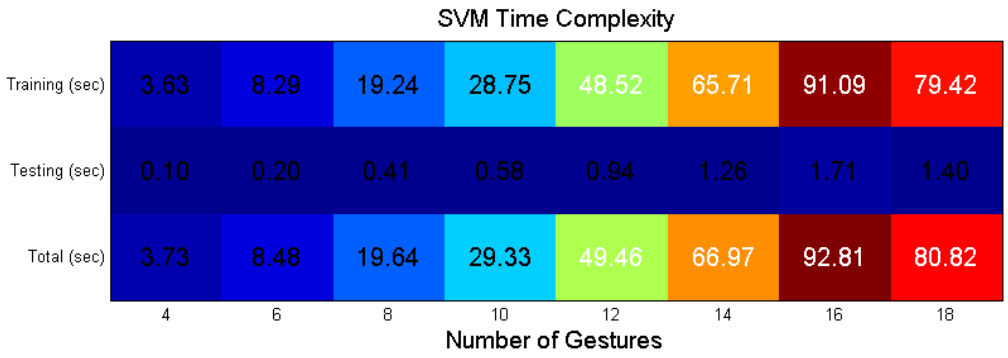


*Figure 51: SVM Time Complexity*

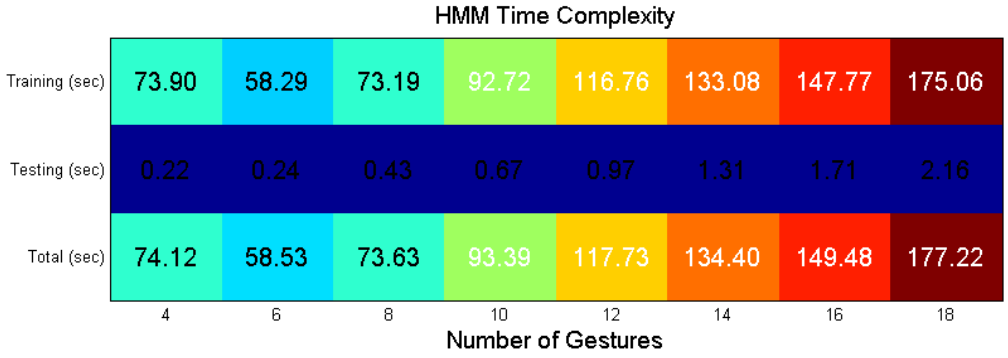


*Figure 52: HMM Time Complexity*

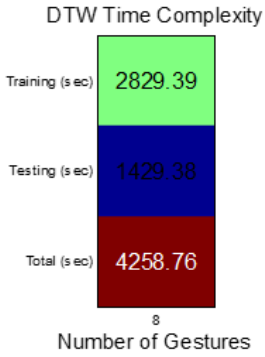


*Figure 53: DTW Time Complexity*

The second set of parameters to compare amongst the methods are the ACVR, ARR, and APR; of these the ACVR is the most important as it provides a quantitative measure of the method's power to properly classify a gesture class. The graph below (Figure 54) shows the combined results of these parameters for all three methods. The first thing which should be apparent is that once again the DTW classifier fails in comparison to the SVM and HMM methods. Not only is it's ACVR result a third of the other classifiers but its recall and precision are also extremely low. Together with the

previous time result, it is now painfully obvious how badly the DTW method performs with the Ninapro dataset. On the other hand, both the SVM and HMM optimized models perform very well with the dataset. Different runs of the same tests, show the ACVR for both methods hovers around 95%, this value, although only for 8 classes, is on par with current state of the art gesture classifiers. Furthermore, both the precision and recall ratios for both methods lie above the 90% mark, assuring that individual gestures are not only properly labeled but also that there aren't a large number of false positives.

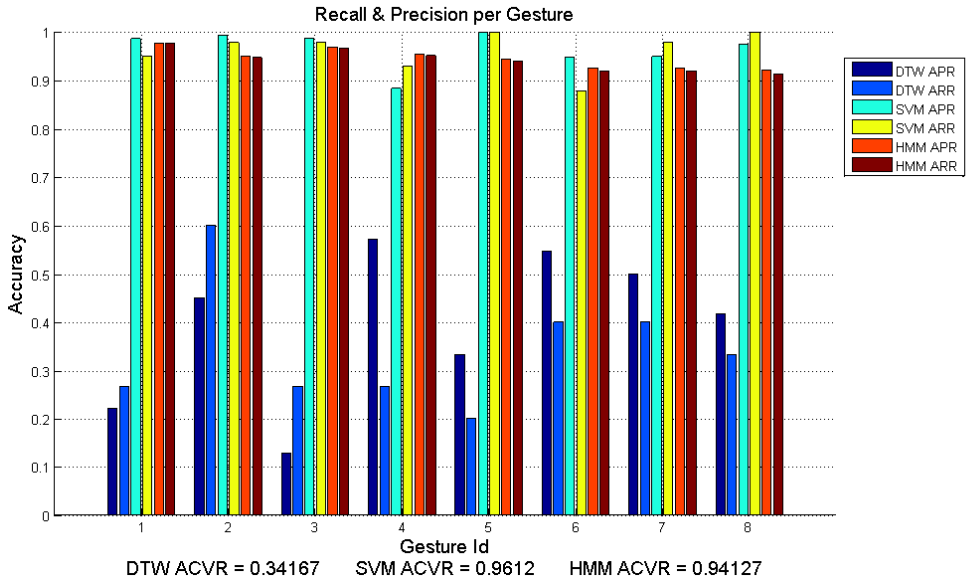


*Figure 54: Overall Classifier Performance*

By looking at both the ACVR and time results, the ultimate conclusion of the tests completed show that the HMM classifier is the ideal choice for the gesture recognition when using the Ninapro EMG dataset.

## 6.4 Achievement

Ultimately three gesture classifiers were designed for classification of EMG data collected in the Ninapro dataset. These classifiers were tested and optimized for classification while taking into consideration the noisiness of the data and while striving for the most scientific approach which minimizes false assumptions and training randomness. Of these methods, the Hidden Markov Model classifier proved to be the most powerful in terms of maximizing cross validation accuracy while minimizing

training and classification times. Altogether, this work paves a roadmap for the kinds of issues and parameters to look for when dealing with EMG data. In a continuing work, this roadmap might be reused in order to find the optimal classifier for other kinds of data, or in order to continue down the path and arrive at a product which might be usable by an end user.

## 6.5 Future work

There are a number of continuations of this work which would allow for the extended use of a gesture classifier while also improving the understanding of a system. First, continuing work will concentrate on using force regression to predict the intended force of grasp. By using the EMG data which contains activation patterns of the muscle, it might also be possible to capture the intended force of the subject. Furthermore, through the use of linear and perhaps non-linear regression, this force information which is hidden in the EMG signals might be able to be transferred to a prosthetic, transforming gesture classification from a discrete domain to a system capable of continuous use. Such an examination would require the same approach as was followed in this work, starting with data collection and representation, and ending with prediction and application. The second path which will be explored is the transformation of the current HMM system into one that is capable of working in real time. This means reducing classification times to an amount of time where lag is not an issue for a user. This also means locating the correct sensors and choosing sensor locations (be it by following the Ninapro instructions or performing a separate experiment). This particular follow up test, was very tempting to approach in this work, however, such an undertaking would have been outside the scope of what was intended. Third, the author is also interested in pursuing the use of independent component analysis on the EMG signals. This is a path which combined with gesture classification, and force regression, would allow for an increased number of degrees of freedom, as well as more articulate control of a prosthetic or robotic arm. Finally, with the understanding that machine learning is a growing field, continuing work must also include the continuous search for more powerful classifiers which might offer better results in the problem of gesture classification.

## 6.6 Summary

The final chapter of this thesis serves as a conclusion of the work undertaken. Structuring these concluding remarks has been done by first presenting previous classification results using the Ninapro dataset, and comparing these results to each of the three learning methods. Each of these methods were then compared amongst themselves for accuracy as well as implementation and computational complexity. Ultimately, the overall achievements were also covered as well as future work which would supplement and expand this system.

# References


[1] J. Strickland, "The Sign Language Alphabet," *How Stuff Works*, 2007. [Online]. Available: http://people.howstuffworks.com/sign-language2.htm.

[2] S. A. R. Tidwell S. Karlaputi, R. Akl, K. Kavi and D. Struble, "Evaluating the feasibility of EMG and bend sensors for classifying hand gestures," in *Proceedings of the International Conference on Multimedia and Human Computer Interaction (MHCI-13)*, 2013.

[3] A. Esquenazi, "Amputation rehabilitation and prosthetic restoration. From surgery to community reintegration," *Disabil. Rehabil.*, vol. 26, no. 14–15, pp. 831–836, Jan. 2004.

[4] A. Suberbiola, E. Zulueta, J. Lopez-Guede, I. Etxeberria-Agiriano, and B. Caesbroeck, "Arm Orthosis/Prosthesis Control Based on Surface EMG Signal Extraction," in *Hybrid Artificial Intelligent Systems*, vol. 8073, J.-S. Pan, M. Polycarpou, M. Woźniak, A. P. L. F. Carvalho, H. Quintián, and E. Corchado, Eds. Springer Berlin Heidelberg, 2013, pp. 510–519.

[5] M. T. Wolf, C. Assad, M. T. Vernacchia, J. Fromm, and H. L. Jethani, "Gesture-based robot control with variable autonomy from the JPL BioSleeve," in *2013 IEEE International Conference on Robotics and Automation (ICRA 2013), Karlsruhe, Germany, May 6-10, 2013*, 2013.

[6] N. M. Kakoty and S. M. Hazarika, "Bio-Signals Controlled Prosthetic Hand," *Natl. Conf. Des. Manuf. Issues Automot. Allied Ind. IPRoMM*, 2009.

[7] J. Rosenvang and R. Horup, "Towards Intuitive Control of Simultaneous Movements and Force Estimation for Myoelectric Prostheses," Aalborg University, 2012.

[8] S. Du, "Feature Extraction for Classification of Perhensile Electromyograhy Patterns," San Diego State University, 2003.

[9] J. L. Hernandez-Rebollar, R. W. Lindeman, and N. Kyriakopoulos, "A multi-class pattern recognition system for practical finger spelling translation," in *Multimodal Interfaces, 2002. Proceedings. Fourth IEEE International Conference on*, 2002, pp. 185–190.

[10] C. A. M. Wolf A. Soica, K. You, H. Jethani, M. Vernacchia, J. Fromm, and Y. Iwashita, "Decoding Static and Dynamic Arm and Hand Gestures from the JPL BioSleeve," in *Proceedings IEEE Aerospace Conference*, 2013.

[11] M. Atzori, A. Gijsberts, S. Heynen, A. M. Hager, O. Deriaz, P. van der Smagt, C. Castellini, B. Caputo, and H. Muller, "Building the Ninapro database: A resource for the biorobotics community," in *Biomedical Robotics and Biomechatronics (BioRob), 2012 4th IEEE RAS & EMBS International Conference on*, 2012, pp. 1258–1265.

[12] A. Gijsberts, M. Atzori, C. Castellini, H. Muller, and B. Caputo, "The Movement Error Rate for Evaluation of Machine Learning Methods for sEMG-based Hand Movement Classification," *Neural Syst. Rehabil. Eng. IEEE Trans.*, vol. PP, no. 99, p. 1, 2014.

[13] "ThalmicLabs." [Online]. Available: https://www.thalmic.com/en/myo/. [Accessed: 04-Aug-2014].

[14] P. Zhou, M. M. Lowery, K. B. Englehart, H. Huang, G. Li, L. Hargrove, J. P. a Dewald, and T. a Kuiken, "Decoding a new neural machine interface for control of artificial limbs.," *J. Neurophysiol.*, vol. 98, no. 5, pp. 2974–82, Nov. 2007.

[15] G. Li, "Electromyography Pattern-Recognition-Based Control of Powered Multifunctional Upper-Limb Prostheses," in *Advances in Applied Electromyography*, J. Mizrahi, Ed. 2011.

[16] T. Pylv and T. Pylvänäinen, "Accelerometer Based Gesture Recognition Using Continuous HMMs," in *Pattern Recognition and Image Analysis*, vol. 3522, J. Marques, N. Pérez de la Blanca, and P. Pina, Eds. Springer Berlin Heidelberg, 2005, pp. 639–646.

[17] N. E. Gillian, "Gesture Recognition for Musician Computer Interaction," Queen's University Belfast, Ireland, 2011.

[18] M. Wöllmer, M. Al-Hames, F. Eyben, B. Schuller, and G. Rigoll, "A multidimensional dynamic time warping algorithm for efficient multimodal fusion of asynchronous data streams," *Neurocomputing*, vol. 73, no. 1–3, pp. 366–380, 2009.

[19] I. Koprinska, "Feature selection for brain-computer interfaces," *New Front. Appl. Data Min.*, 2010.

[20] D. Tkach, H. Huang, and T. a Kuiken, "Study of stability of time-domain features for electromyographic pattern recognition.," *J. Neuroeng. Rehabil.*, vol. 7, p. 21, Jan. 2010.

[21] C. Xiang, Z. Xu, Z. Zhang-Yan, Y. Ji-Hai, V. Lantz, W. Kong-Qiao, X. Chen, X. Zhang, Z.-Y. Zhao, J.-H. Yang, and K.-Q. Wang, "Hand Gesture Recognition Research Based on Surface EMG Sensors and 2D-accelerometers," in *Wearable Computers, 2007 11th IEEE International Symposium on*, 2007, pp. 11–14.

[22] N. S. Rekhi, A. S. Arora, S. Singh, and D. Singh, “Multi-Class SVM Classification of Surface EMG Signal for Upper Limb Function,” in *Bioinformatics and Biomedical Engineering , 2009. ICBBE 2009. 3rd International Conference on*, 2009, pp. 1–4.

[23] M. V Liarokapis, P. K. Artemiadis, P. T. Katsiaris, and K. J. Kyriakopoulos, “Learning task-specific models for reach to grasp movements: Towards EMG-based teleoperation of robotic arm-hand systems,” in *Biomedical Robotics and Biomechatronics (BioRob), 2012 4th IEEE RAS & EMBS International Conference on*, 2012, pp. 1287–1292.

[24] Z. Xu, C. Xiang, L. Yun, V. Lantz, W. Kongqiao, Y. Jihai, X. Zhang, X. Chen, A. Member, Y. Li, K. Wang, and J. Yang, “A Framework for Hand Gesture Recognition Based on Accelerometer and EMG Sensors,” *Syst. Man Cybern. Part A Syst. Humans, IEEE Trans.*, vol. 41, no. 6, pp. 1064–1076, 2011.

[25] G. A. Garcia, R. Okuno, and K. Azakawa, “A decomposition algorithm for surface electrode-array electromyogram,” *Eng. Med. Biol. Mag. IEEE*, vol. 24, no. 4, pp. 63–72, 2005.

[26] N. Shapiro, “Motor Unit Recruitment Strategies During Deep Muscle Pain,” *The alchemist*. [Online]. Available: http://natchem.wordpress.com/2009/11/23/motor-unit-recruitment-strategies-during-deep-muscle-pain/.

[27] A. Zeghbib, *Forearm Surface EMG Signals Recognition and Muscoloskeletal System Dynamics Identification Using Intelligent Computational Methods*. 2007, p. 229.

[28] J. Kim, S. Mastnik, E. Andr, and #233, “EMG-based hand gesture recognition for realtime biosignal interfacing,” *Proceedings of the 13th international conference on Intelligent user interfaces*. ACM, Gran Canaria, Spain, pp. 30–39, 2008.

[29] G. R. Naik, D. K. Kumar, V. P. Singh, and M. Palaniswami, “Hand gestures for HCI using ICA of EMG,” *Proceedings of the HCSNet workshop on Use of vision in human-computer interaction - Volume 56*. Australian Computer Society, Inc., Canberra, Australia, pp. 67–72, 2006.

[30] A. S. Mannini  Angelo Maria, A. Mannini, and A. M. Sabatini, “Machine Learning Methods for Classifying Human Physical Activity from On-Body Accelerometers,” *Sensors*, vol. 10, no. 2, pp. 1154–1175, Jan. 2010.

[31] M. Müller, “Dynamic Time Warping,” in *Information Retrieval for Music and Motion*, Springer Berlin Heidelberg, 2007, pp. 69–84.

[32] C. R. Souza, “Kernel Functions for Machine Learning Applications,” 2010. [Online]. Available: http://crsouza.blogspot.com/2010/03/kernel-functions-for-machine-learning.html. [Accessed: 08-Jan-2014].

[33] R. N. Khushaba, S. Kodagoda, M. Takruri, and G. Dissanayake, “Toward improved control of prosthetic fingers using surface electromyogram (EMG) signals,” *Expert Syst. Appl.*, vol. 39, no. 12, pp. 10731–10738, 2012.

[34] B. Direito, J. Duarte, and C. Teixeira, “Feature selection in high dimensional EEG features spaces for epileptic seizure prediction,” *Proc. 18th IFAC …*, 2011.

[35] R. Chowdhury, M. Reaz, M. Ali, A. Bakar, K. Chellappan, and T. Chang, “Surface Electromyography Signal Processing and Classification Techniques,” *Sensors*, vol. 13, no. 9, pp. 12431–12466, 2013.

[36] A. Phinyomark, “A novel feature extraction for robust EMG pattern recognition,” *arXiv Prepr. arXiv …*, vol. 1, no. 1, pp. 71–80, 2009.

[37] A. Hussein Ali, “An Investigation of Electromyographic (EMG) Control of Dextrous Hand Prostheses for Transradian Amputees,” Ieee, 2013.

[38] A. D. C. Chan and G. C. Green, “Myoelectric control development toolbox,” *Proc. 30th Conf. Can. Med. Biol. Eng. Soc.*, vol. 1, pp. M0100–1, 2007.

[39] A. Shakoor, T. May, and N. Van Schijndel, “Soft computing based feature selection for environmental sound classification,” Blekinge Institute of Technology, 2010.

[40] S. Chakrabarti, B. Dom, R. Agrawal, and P. Raghavan, “Scalable feature selection, classification and signature generation for organizing large text databases into hierarchical topic taxonomies,” *VLDB J. Int. J. Very Large Data Bases*, vol. 7, no. 3, pp. 163–178, Aug. 1998.

[41] S.-Y. Kung and M.-W. Mak, “Feature Selection for Genomic and Proteomic Data Mining,” in *Machine Learning in Bioinformatics*, Y. Pan and A. Y. Zomaya, Eds. JOHN WILEY & SONS, INC., 2009, pp. 1–46.

[42] I. Guyon, “An Introduction to Variable and Feature Selection,” *J. Mach. Learn. Res.*, vol. 3, pp. 1157–1182, 2003.

[43] J. B. MacQueen, “Some Methods for classification and Analysis of Multivariate Observations,” in *Proceedings of 5-th Berkeley Symposium on Mathematical Statistics and Probability*, 1967, pp. 281–297.

[44] T. T. Swee, A. K. Ariff, S. H. Salleh, S. Siew Kean, and H. Leong Seng, “Wireless data gloves Malay sign language recognition system,” in *Information,*

*Communications & Signal Processing, 2007 6th International Conference on*, 2007, pp. 1–4.

[45] X. Chen and Z. J. Wang, "Pattern recognition of number gestures based on a wireless surface EMG system," *Biomed. Signal Process. Control*, vol. 8, no. 2, pp. 184–192, Mar. 2013.

[46] C. Chang and C. Lin, "LIBSVM: a library for support vector machines," *ACM Trans. Intell. Syst. ...*, vol. 2, no. 3, pp. 1–39, 2011.

[47] C.-J. Lin, "Errata to 'A comparison of methods for multiclass support vector machines'.," *IEEE Trans. Neural Netw.*, vol. 13, no. 4, pp. 1026–7, Jan. 2002.

[48] C. Hsu, C. Chang, and C. Lin, "A Practical Guide to Support Vector Classification," vol. 1, no. 1, pp. 1–16, 2010.

[49] M. Atzori, "Characterization of a Benchmark Database for Myoelectric Movement Classification," *Neural Syst. Rehabil. Eng.*, vol. PP, no. 99, 2014.

# Appendix A: Gesture Dictionary

Experiment Setup, A. Gijsberts, M. Atzori, C. Castellini, H. Muller, and B. Caputo, "The Movement Error Rate for Evaluation of Machine Learning Methods for sEMG-based Hand Movement Classification," *Neural Syst. Rehabil. Eng. IEEE Trans.*, vol. PP, no. 99, p. 1, 2014.
Used under fair use, 2014.

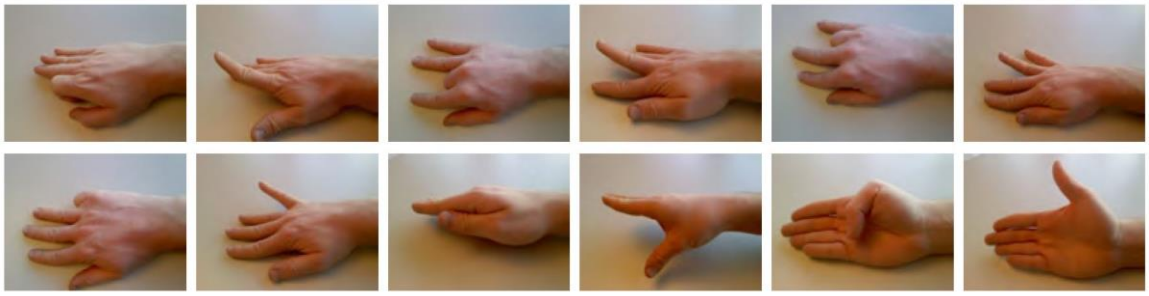

(a) Basic movements of the fingers (flexions and extensions).

(b) Isometric, isotonic hand configurations ("hand postures").

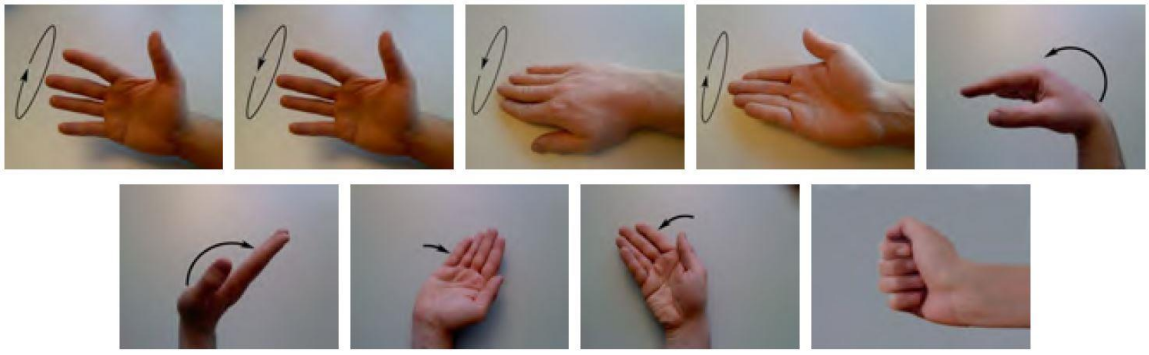

(c) Basic movements of the wrist.

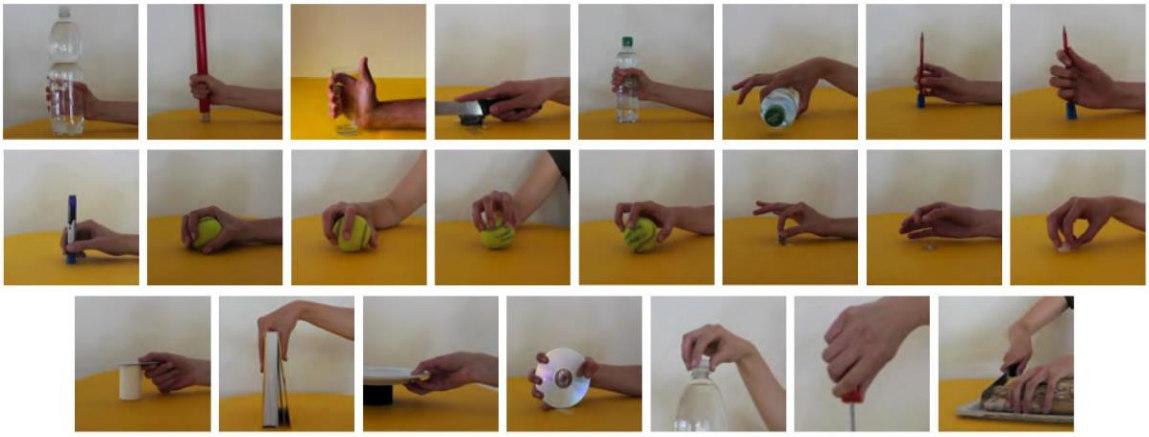

(d) Grasping and functional movements.

DESCRIPTION OF THE 9 FORCE PATTERNS.

| # | Description |
|---|---|
| 1 | Flexion of the little finger |
| 2 | Flexion of the ring finger |
| 3 | Flexion of the middle finger |
| 4 | Flexion of the index finger |
| 5 | Abduction of the thumb |
| 6 | Flexion of the thumb |
| 7 | Flexion of the index and little finger |
| 8 | Flexion of the ring and middle finger |
| 9 | Flexion of the index finger and the thumb |

| | | |
|---|---|---|
| Hand and wrist movements | 1 | Thumb up |
| | 2 | Extension of index and middle finger while flexing others (cf. "V-sign") |
| | 3 | Flexion of ring and little finger while extending others |
| | 4 | Thumb opposing base of little finger |
| | 5 | Abduction of the fingers |
| | 6 | Fingers flexed together in fist |
| | 7 | Pointing index |
| | 8 | Adduction of extended fingers |
| | 9-10 | Wrist supination and pronation (rotation axis through the middle finger) |
| | 11-12 | Wrist supination and pronation (rotation axis through the little finger) |
| | 13-14 | Wrist flexion and extension |
| | 15-16 | Wrist radial and ulnar deviation |
| | 17 | Wrist extension with closed hand |
| sps and functional movements | 18-19 | Large and small diameter grasp |
| | 20-21 | Fixed hook and index finger extension grasp |
| | 22 | Medium wrap |
| | 23-24 | Ring and prismatic four fingers grasp |
| | 25-26 | Stick and writing tripod grasp |
| | 27-29 | Power, three finger, and precision sphere grasp |
| | 30-32 | Tripod, prismatic, and tip pinch grasp |
| | 33-35 | Quadpod, lateral, and parallel extension grasp |
| | 36 | Extension type grasp |
| | 37 | Power disk grasp |
| | 38 | Open a bottle with a tripod grasp |

## Appendix B: EMG Features

| Feature | Mathematical Representation |
|---|---|
| Integrated EMG (IEMG) | $IEMG = \sum_{n=1}^{N} \lvert x_n \rvert$<br>Where x is a EMG signal and N is the length of that signal |
| Mean Absolute Value (MAV) | $MAV = \frac{1}{N}\sum_{n=1}^{N} \lvert x_n \rvert$ |
| Modified Mean Absolute Value 1 (MMAV1) | $MMAV1 = \frac{1}{N}\sum_{n=1}^{N} w_n \lvert x_n \rvert$<br>$w_n = \begin{cases} 1, & if\ 0.25N \le n \le 0.75N \\ 0.5, & otherwise \end{cases}$ |
| Modified Mean Absolute Value 2 (MMAV2) | $MMAV2 = \frac{1}{N}\sum_{n=1}^{N} w_n \lvert x_n \rvert$<br>$w_n = \begin{cases} 1, & if\ 0.25N \le n \le 0.75N \\ \frac{4n}{n}, & if\ 0.25N \le n \\ \frac{4(n-N)}{n}, & if\ 0.75N \le n \end{cases}$ |
| Single Square Integral (SSI) | $SSI = \sum_{n=1}^{N} \lvert x_n \rvert^2$ |
| Variance of EMG (VAR) | $Sample\ Variance = \frac{1}{N-1}\sum_{n=1}^{N} (x_n - \bar{x})^2$ |
| Root Mean Square (RMS) | $RMS = \sqrt{\frac{1}{N-1}\sum_{n=1}^{N} (x_n - \bar{x})^2}$ |
| Waveform Length (WL) | $WL = \sum_{n=1}^{N} \lvert x_{n+1} - x_n \rvert$ |

| | |
|---|---|
| Willison Amplitude (WAMP) | $$WAMP = \sum_{n=1}^{N} f\lvert x_{n+1} - x_n \rvert$$ Where $$f = \begin{cases} 1, & if\ x \geq threshold \\ 0, & otherwise \end{cases}$$ |
| Log Detector (LOG) | $$LOG = e^{\frac{1}{N}\sum_{n=1}^{N} log\lvert x_n \rvert}$$ |
| Slope Sign Change (SSC) | $$SSC = \sum_{n=2}^{N} f[(x_n - x_{n-1}) \times (x_n - x_{n+1})]$$ Where $$f = \begin{cases} 1, & if\ x \geq threshold \\ 0, & otherwise \end{cases}$$ |
| Zero Crossing (ZC) | $$ZC = \sum_{n=1}^{N-1} [sgn(x_n \times x_{n+1}) \cap \lvert x_n - x_{n+1} \rvert \geq threshold]$$ Where $$f = \begin{cases} 1, & if\ x \geq threshold \\ 0, & otherwise \end{cases}$$ |
| Multi Scale Amplitude Modulation Frequency Modulation (AM-FM) | $$f(k) = \sum_{n=2}^{N} a_n(k) \cos \emptyset_n(k)$$ Here n = 1, 2,…M indexes the AM–FM components, an represents the nth instantaneous amplitude, and ϕn represents the nth instantaneous phase. Here, AM–FM components are extracted over a dyadic filter bank. |